UNIVERSITY OF CALIFORNIA,
IRVINE

Simulation and Analysis of Reactive Power Compensation Methods in Presence of Solar Distributed Generation and Development of Optimal Capacitor Placement and Sizing

THESIS

submitted in partial satisfaction of the requirements
for the degree of

MASTER OF SCIENCE

in Electrical and Computer Engineering

by

Daniel Gebbran Cons Bacilla Ferreira

Thesis Committee:
Professor Keyue Smedley, Chair
Professor Michael M. Green
Professor Filippo Capolino

2017

DEDICATION

To my loving wife, Rosemary, without whom my accomplishments would mean nothing and would not be possible; for being the best friend I could ever wish for, for having patience, for always keep pushing me beyond my limits, and for being my kindred soul;

To all my professors and teachers, who each inspired and touched me in their own manners, for that inspiration has always driven me forward;

To both my parents, Kathi and Ciro, for being the best teachers I had when growing up; who taught me goodness.

To Sirius

TABLE OF CONTENTS

LIST OF FIGURES

LIST OF GRAPHS

LIST OF TABLES

ACKNOWLEDGMENTS

First of all, I would like to express my gratitude towards my advisor, Professor Keyue Smedley, for her support since I first contacted her, and for her orientation. Her Power Electronics Laboratory at UCI provides a rich environment for research to thrive, as well as her expertise on both application and research topics.

This thesis has only been made possible with the support of CNPq, the Brazilian National Council of Scientific and Technological Development, which enabled the pursuit of my graduate studies by the Science Without Borders scholarship. They have supported on my undergrad studies by providing an exchange scholarship to study Electrical Power Engineering in Denmark, which has then enabled and inspired me to continue pursuing my studies on remarkable environments - as the University of California Irvine.

Last but not least, I would like to thank Professor Michael M. Green and Professor Fillippo Capolino to kindly accept to be part of my thesis committee.

ABSTRACT OF THE THESIS

Simulation and Analysis of Reactive Power Compensation Methods in Presence of Solar Distributed Generation and Development of Optimal Capacitor Placement and Sizing

By

Daniel Gebbran Cons Bacilla Ferreira

Master of Science in Electrical and Computer Engineering

University of California, Irvine, 2017

Professor Keyue Smedley, Chair

The electrical power grid is the biggest man-made system, and one of the most complex ones. This system has been up and evolving from about a century into the large connected system we have today. However, innovations are very few in recent years, and it becomes more outdated as days go by. Moreover, we need to modify the operational status quo - not environmentally friendly because of its predominant coal-based generation. Investigation of the grid's behavior and study of control techniques under new scenarios, such as renewable energy generation, is needed to update the grid to cope with new challenges brought by implementation of modern technologies enhancing our power systems.

In this thesis, effects of Reactive Power will be discussed, VAR compensation techniques such as static, switched capacitor banks and static VAR compensators are simulated on a grid with high solar energy penetration. Two different software are used to simulated a 12.47 kV, 7 MW circuit, and VAR compensation is studied in conjunction with

load curves. The VAR Compensation methods are effectively employed, and discussions made regarding their effects.

A new technique of optimal capacitor placement and sizing for losses reduction is developed, using power flow optimization and graphical tools to achieve the most efficient and effective place and size for banks placement. Using easy-to-implement steps, it enables losses and costs reduction , increasing grid's efficiency. The validity of the approach is tested in the same grid previously studied, confirming its functioning and effectively reducing over 5% of circuit losses.

1. INTRODUCTION

Generation, transmission and distribution of electrical power is vital for every country to function properly. Not only that, but there is also a need to continuously increase power generation, since it is only natural that more energy is required as population grows and our civilization advances [1]. Moreover, the increase in power generation is roughly proportional to the growth of gross domestic product (GDP) [2]. Even though efficiency has been improving throughout the years [3], and will continue this trend [4], it is true that most nations will require more power to be generated.

In some areas, most of the electricity generated comes from thermal power plants [5]. In other areas, where hydroelectric power is abundant, even then the capacity of the rivers is close to its maximum capacity [6].

Therefore, for the electricity generation to grow jointly with demand, a choice must be made in every region: to build more of the traditional, pollutant fossil fuel-based power generators, which are neither environmentally friendly nor sustainable, or to build, instead, other forms of generation, such as solar, wind, and small hydro.

In addition to that, we need to shift the trend of carbon-based power as soon as possible, since a slow shift is prone to continue worsening its environmental results [5]. The impacts of traditional generation have had over the last century are significant, and up to today, electricity generation represents more than 25.9% of CO_2 emissions. Combined with transportation, they represent more than one third of the global CO_2 emissions [6].

This means that, in addition to increasing efficiency throughout all areas and operations, we also need to concern ourselves with developing and applying new methods,

equipment, and methodologies, besides reviewing our existing technologies. Combining these efforts is essential to cope with the necessary changes.

Even with technology increasing at a fast pace, we do not see these advancements reflected upon the electric grid. Most of our infrastructure is outdated, and even more, the whole concept of it has been unchanged for decades [7]. Centralized generation, unidirectional power flow, and AC transmission and distribution systems are some of the characteristics that, up to recently, were taken as immutable, inherent to any power system.

This means there is little room for improvement as is. For instance, the user has little to no information regarding its consumption [7], which blinds him to understanding and coping with this trend by individual actions.

Often cited, the smart grid is an enabler of this new era of electricity, where each component has an influence that is taken in account, and in which the old paradigms are not predominant anymore.

Combined with distributed generation, the renewables require bidirectional power flow, which brings both more flexibility and more complexity to today's grid. In here, mention to distributed generation may take many forms, such as solar power plants, solar roof tops in residential or commercial buildings, wind power plants, and biomass power plants, installed in individual farms or as small scale, regional power plants.

However, by increasing the complexity of our grid, we must cope with that by new means of control and equipment which were not thought of up to today, given they were not necessary, not existing, or both. For instance, the availability of solar or wind power is dependent upon climate conditions, and they have unpredictable, fast changes throughout their whole operation.

To deal with these, we need strategies that include this kind of situations, as well as the proper equipment. In this context, the power electronics field comes in as a key technology [8], capable of making the bridge between the two worlds. Equipping our grid with highly responsive, capable power electronics equipment, and performing the correct planning and execution, we can cope with the high requirements necessary for the operation of this new grid.

On the bright side, many companies, utilities and researchers have been occupied with such new ways of modifying or improving the traditional unidirectional, centralized electrical power grid. That is a huge and extensive task, but with combined effort this challenge can be tackled [9].

Other applications can be cited among various lines – and many different strategies to bypass the intermittency of the renewable energy sources are getting more and more common, and applications are already up and running. For example, Plug-In Electrical Vehicles (PEV) and Plug-In Hybrids Electric Vehicles (PHEV) have been undergoing increasing market share [10], and offer a flexible component for the electrical grid side [11][12], and a more environmentally friendly solution for transportation.

1.1. Thesis objectives

Efforts have been made towards renewing the Electrical Power System and many technologies are already available, however their effectiveness in large-scale usage and joint efficiency is still an area lacking in research and implementation.

For that sake, this thesis shall cover usage of Reactive Power Compensation methods, also known as VAR compensation, by using two different power systems simulation tools, ETAP and OpenDSS, while employing a real power system, provided by

Southern California Edison. An initial analysis of the static system will outline the properties and characteristics of given system, and a more comprehensive simulation including solar power production intermittency and load demand curves will follow up, when strategies will be discussed for use in this real scenario.

By utilizing VAR compensation methods in a system where Distributed Generation is in effect, we study control strategies that promote usage of renewable power generation, integrating its possibilities within the grid whilst also improving the energy quality by maintaining a high standard in the operation.

Afterwards, a new method for capacitor bank placement, sizing and switching coordination is introduced. By making use of the same tools in addition to graphical representations, a different and reproducible approach is developed, so to enable engineers and operators to review or design new systems without needing complex theory.

Lastly, a chapter encompasses usage of another VAR compensation technique, a SVC, to lessen some of the voltage fluctuation effects. Different sizes and positions are tested and, again, an optimal range for placement is studied for its implementation.

2. BACKGROUND

Not all electricity generated reaches the final consumers. In fact, for our electrical grid to properly work, its components need some form of energy. For instance, cables dissipate power in form of heat, proportionally to their resistance and the square of the current going through them.

This means the further our energy has to move, the more losses we have to cope with. That is another argument in favor of distributed generation, since having generation closer to where demand is, means also increasing the overall efficiency of our system.

In average, more than 7% of the energy is dissipated in this process [13]. That means any improvement we achieve on distribution and transmission, is directly reflected upon losses and, thus efficiency.

2.1. Reactive Power Demand

A variety of loads demand only real power, but many others also require a reactive power *Q*, (Volt Ampere reactive – VAR), component in addition to its regular, active power *P* (Watt – W). The sum of their squares is the magnitude of the apparent power *S* (Volt Ampere – VA):

$$P^2 + Q^2 = S^2 \quad (1)$$

Their relationship is given by the Power Triangle, shown on Figure 1.

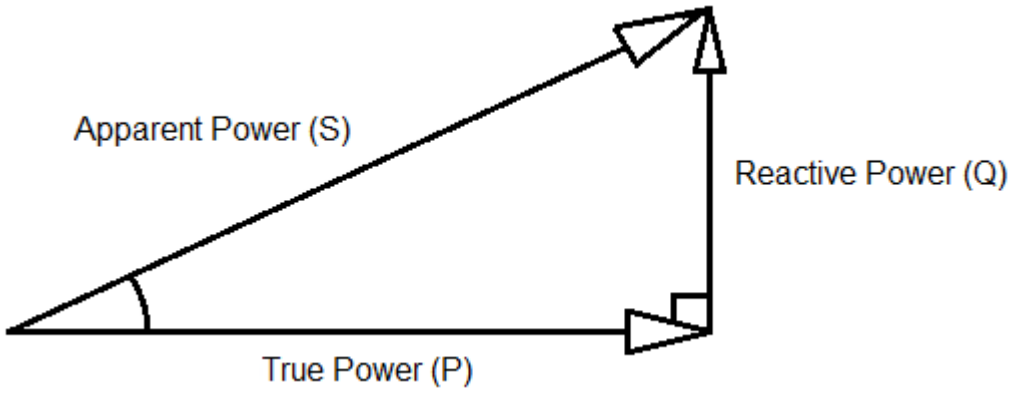

Figure 1: Power Triangle

The denoted angle is the phase angle θ, which is the phase shift between voltage and current. Also, if we have no harmonics, the Power Factor PF is:

$$PF = \cos \theta \tag{2}$$

It establishes how much reactive power we are generating; if cos θ = 1, S = P and no reactive power is being generated, which is the best condition for most scenarios, as it will be explained in the next section. On the other hand, if cos θ = 0, then S = Q.

The apparent power, given by Eq. N, is so called since it is obtained by multiplying the voltage phasor **V** and its complex conjugate current, **I***, both observables entities of fairly easy acquisition. The phasor **S** is composed of its magnitude, given by Eq. N-2, and its angle θ.

$$\mathbf{S} = \mathbf{V}\mathbf{I}^* \tag{3}$$

The real power P is what generates work. Loads with real power are actively consuming energy through their resistance, transforming electricity into other energy forms, such as heating devices.

On the other hand, reactive power does not generate work, but is essential for the proper functioning of various AC devices. Equipment such as transformers, motors, transmission lines, all have reactance in addition to their resistance, which then generates inductive reactive power – also called lagging reactive power – upon imposition of an external voltage for their functioning.

This is a natural property of these equipment; however, it must be addressed or may bring harm to the system's functioning, as seen on the next session.

2.2. Losses in Transmission and Distribution Systems

The lines and cables have resistivity R, and they have power losses equivalent to:

$$P = RI^2 \tag{4}$$

In addition to these losses, transformers also have the same conductor losses as lines and cables, and additionally, magnetic losses given by their internal arrangement [14].

In the normal operation of the AC power grid, reactive power is both required and generated. While for residential consumers that is only a very small portion of its loads, for commercial and even more industrial customers, it encompasses a considerable parcel of their total power. The power factor of equipment may vary considerably, such as motors with so called low PF, around 0.6. On power systems, these must be accounted, as well as effects of the grids devices.

If we let these loads unattended, the resulting power factor of a given consumer might be low enough as to cause problems on the electrical grid. As the reactive power flow

increases, we also have witness a voltage drop in the network [15]. This is bad, since we desire our system to remain as close to nominal voltage in normal operation status. Also, by having more current to supply such reactive power, we also have to overcome more losses, which then cause our system to be even less efficient.

2.3. VAR Compensation Methods

To supply this reactive power, various methods are available nowadays.

Early in the past century, reactive power compensations were done by synchronous condensers, which is a synchronous machine adjusted so to generate or absorb reactive power. Previously the most common solution, today they are rarely used due to higher losses, slow response, starting and protective equipment [16].

Later, static capacitor banks became more usual. Up to today, switched capacitors are still a very common solution, capable of providing a big quantity of reactive power demanded by the system. Unlike earlier equipment, todays are equipped with switching features that enable the correction of the PF in the correct range, without exceeding the amount desired and provoking an overvoltage.

More recently, using Power Electronics as an enabler, different solutions capable of handling previously unattended aspects of power regulation became available, including fine adjustment and voltage regulation, power quality, and, also, PF. Different techniques have emerged with the rise of this field, such as Thyristorized VAR Compensators (TVCs) and Self-Commutated VAR Compensators, which include many modern technologies such as static synchronous compensators (STATCOMs), Unified Power Flow Controllers (UPFCs),

and Dynamic Voltage Restorers (DVRs) [16] [17].

3. LOAD FLOW SIMULATION AND ANALYSIS

3.1. Simulation Circuit

For this thesis, a power distribution circuit of Southern California, provided by Southern California Edison [18] is used as a representation of a complex power system, with real behavior and loads.

The given circuit, shown on Figure 2, groups up minor loads throughout all distribution subsystems as major loads, represented as a total of 39 loads, with a total rate of 7 MW and 4.8 MVAR. Most of these loads are three phasic, but two of them are monophasic and four of them are biphasic. Nevertheless, 98.7% of the load is three-phasic, meaning our circuit is well-balanced. Four capacitor banks of 1800 kVAR each are presented in different nodes.

A total of 170 nodes, 90 cables and 36 transmission lines compose the system. The substation provides the point of connection with external energy supply. The system voltage is 12.47 kV, from the substation connection point through each load.

Additionally, two solar power plants of 1.5 and 3.5 MW are present on the system. This fact expands the possibilities of simulation, since it is a representation of a real system with distributed generation. These ratings provide a substantial amount of solar power penetration in the circuit. Seven and three step-up transformers of 210 V/12.47 kV and 500 kVA are present on the solar plants of 3.5 and 1.5 MV, respectively. The total power generated has been distributed equally throughout the three phases.

The total distance from the start to the end of the circuit is 28017 ft, or 8.54 km.

Table 1 shows the distance from the substation to each of the relevant components.

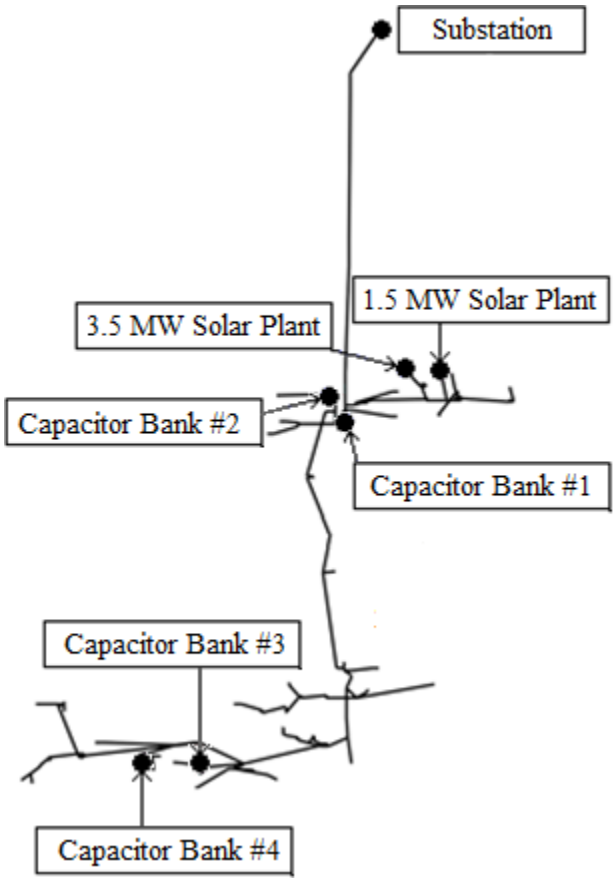

Figure 2: Southern California Edison Power Circuit

Component	Distance from substation (ft)	Distance from substation (m)
Capacitor Bank # 1	10201	3109
Capacitor Bank # 2	11283	3439
Capacitor Bank # 3	23465	7152
Capacitor Bank # 4	24776	7552
1.5 MW Solar Plant	12392	3777
3.5 MW Solar Plant	12066	3678

Table 1: Distance of Relevant Components

3.2 Software Simulation Tool

ETAP 14.1 was selected as one of the Power Systems software to perform the systems' power flow analysis. It offers an enterprise solution for a wide array of power systems applications, capable of handling complex systems.

Figure 3 shows the Graphic User Interface (GUI) representation of SCE's circuit in ETAP.

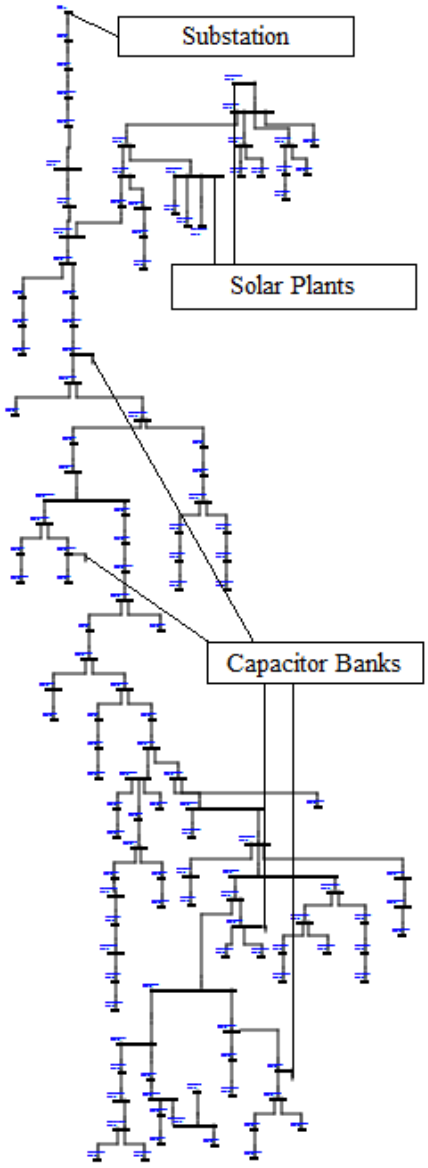

Figure 3: SCE Power Circuit Implemented in ETAP

3.3 VAR Compensation through Capacitor Banks

At first, our simulations will not entail solar generation, as to better demonstrate the effects of reactive power throughout the grid with no further complexity added.

The substation operation mode in our simulation scenario is a Swing mode. This means that it will provide enough power so that the voltage phasor is constant at the power grid terminal, on the point of coupling. In other words, it will take up the slack of the power flows in the system. As the physical system is designed so to provide enough power to the loads, we are not concerned about the system demanding more power than the power grid would otherwise be able to provide. This is, therefore, the real functioning of the power grid.

Voltage level on all buses must be within 95% of its nominal value [19, 20], meaning we must not have a voltage drop under 5% at any bus. Normally, the farther the bus is located, the lower its voltage will be, and all efforts are made so that the last bus is within this limit.

Most buses in our system are at 12.47 kV, which means the voltage must not drop below 11.8465 kV, and only inside the solar plants we have different voltages.

The effects of reactive power described at Chapter 2 can be easily seen by performing an initial simulation using the full nominal load, without any of the capacitor banks connected.

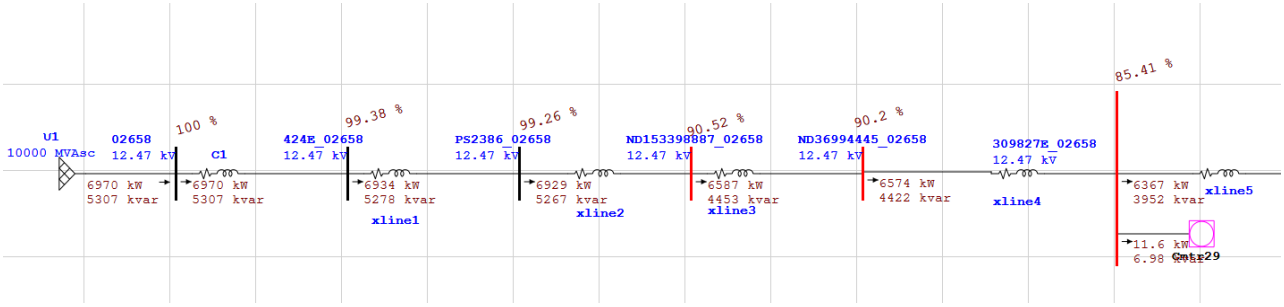

Figure 4: Beginning of Circuit at Initial Simulation

Even though the circuits' current of 406 A is within the limits for the lines (470 and 600 A), the voltage drop is very high from the first bus 02658 towards the next buses. After transmission lines xline2 (3643 ft) and xline4 (2739 ft), there is a substantial decrease in the bus voltage. This agrees with the theory of Chapter 1 and 2, and represents a grave problem for our system, since it is inoperable as is.

If one of the capacitor banks is enabled, we will see a reduction of these effects.

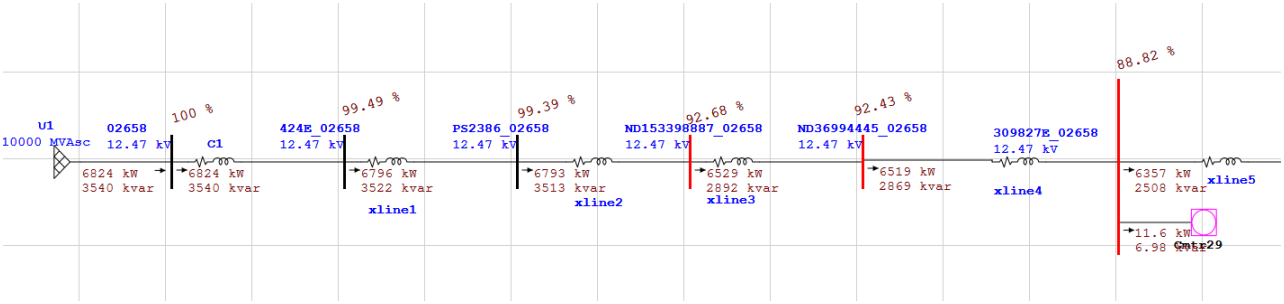

Figure 5: Beginning of Circuit with one bank enabled

However, as each capacitor bank provides 1800 kVAR, a single one will not be able to provide the reactive power for all loads in our system. Using two, instead, we can see the effects diminishing on Figure 5. As we add more capacitor banks, we sum up our results from those different simulations.

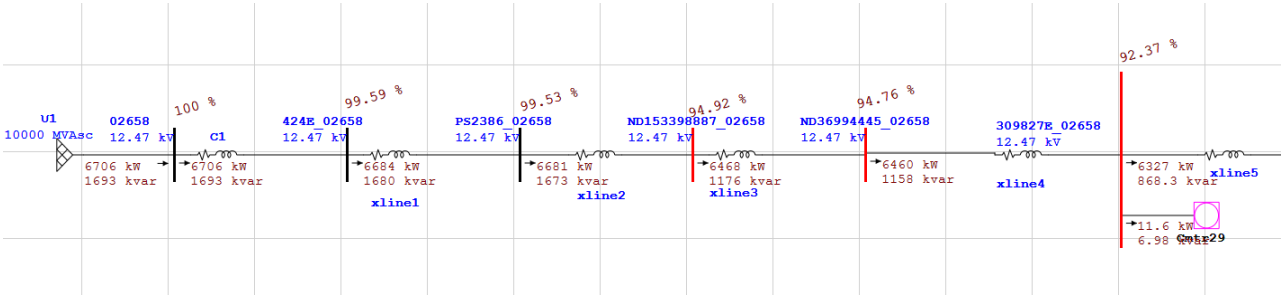

Figure 6: Beginning of Circuit with two capacitor banks

Case #	Capacitor Bank Active	Cable 1 Current (A)	Substation Active Power (kW)	Substation Reactive Power (kVAR)	Highest Voltage on Buses (%)	Lowest Voltage on Buses (%)	Substation Power Factor	Power Losses (kW)
1	None	406	6934	5278	99.38	82.03	0.796	704
2	#1	356	6796	3521	99.49	85.63	0.888	558
3	#2, #3	320	6684	1680	99.59	90.19	0.970	441
4	#1, #3, #4	309	6680	-313	99.71	95.1	0.999 Leading	414
5	All Active	332	6729	-2477	100.35	99.45	0.940 Leading	463

Table 2: Simulation Results with none to four banks enabled

By looking at Table 2, it may be seen that the capacitor banks may provide enough reactive power to supply all the loads on the system. When three or more banks are switched on, there is an excess of kVAR which flows back into the substation, represented by the negative sign in front of its value.

Additionally, we would like to keep the substation PF as close as possible to 1. We can see that cases 1 and 2 have very poor performance regarding this criterion.

At the same time, we see a substantial improvement on the buses' voltage profiles. Graph 1 shows that improvement across all buses. We can see only two of the simulations consistently have profiles over the desired lower limit of 95%, which are with 3 and 4

capacitors.

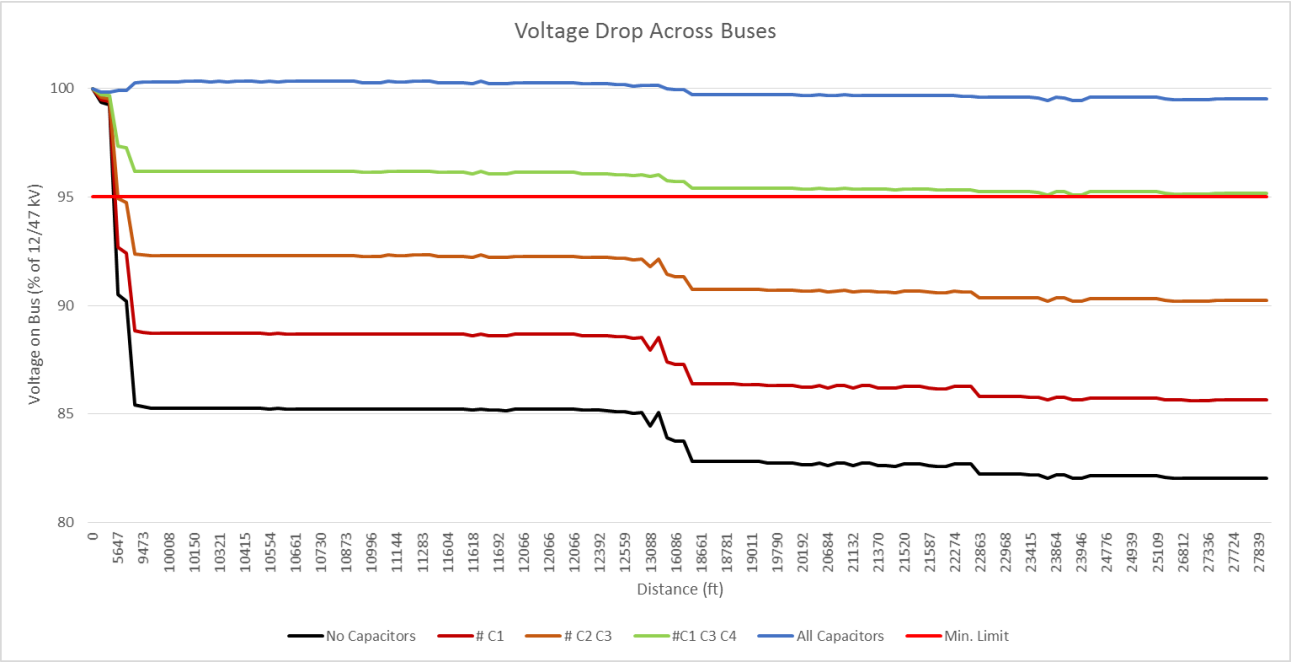

Graph 1: Voltage Drop Across Buses

Table 2 also shows that the input current decreases the most when the internal kVAR generation is close to kVAR demand, which is when three capacitor banks are active. This agrees with the theory from Section 2, since most of the exceeding current which would be required by providing (or absorbing, in case of all capacitor banks active) kVAR to the system.

That makes clear how much Cable 1 would have to be oversized just to handle the additional current. 25% of its current would be just for the sake of reactive power supply, requiring an oversizing - as well as every series-connected component would, such as the five following transmission lines. Taking into account the size and cost of each cable or line, it is clear how costly that would prove to be.

3.4 Effects of Physical Location on VAR Compensation

Next, we would like to investigate what is the best physical placement for our reactive compensators, in particular whether our circuit has requirements as to which capacitors are to be turned on.

To understand what are the effects of different positioning for the capacitor banks - if any, we will simulate all possible cases under nominal load. Therefore, we will be able to compare not only differences based on how many banks are actively contributing to supply the reactive power demand on the circuit, but also where they are located and the relation it promotes within the system.

This means the next simulation will encompass 16 different cases, ranging from no capacitor banks active, to all active, going through all combinations in between: 4 cases with 1, 6 cases with 2 capacitor banks, and 4 cases with 3 banks.

The same parameters and methodology previously described are to be used here as well. Additionally, we are going to measure the reactive power flow at certain key points, detailed in the next page. This way, we will be able to understand the differences in the results, as the kVAR flow will point out the internal effects of each case.

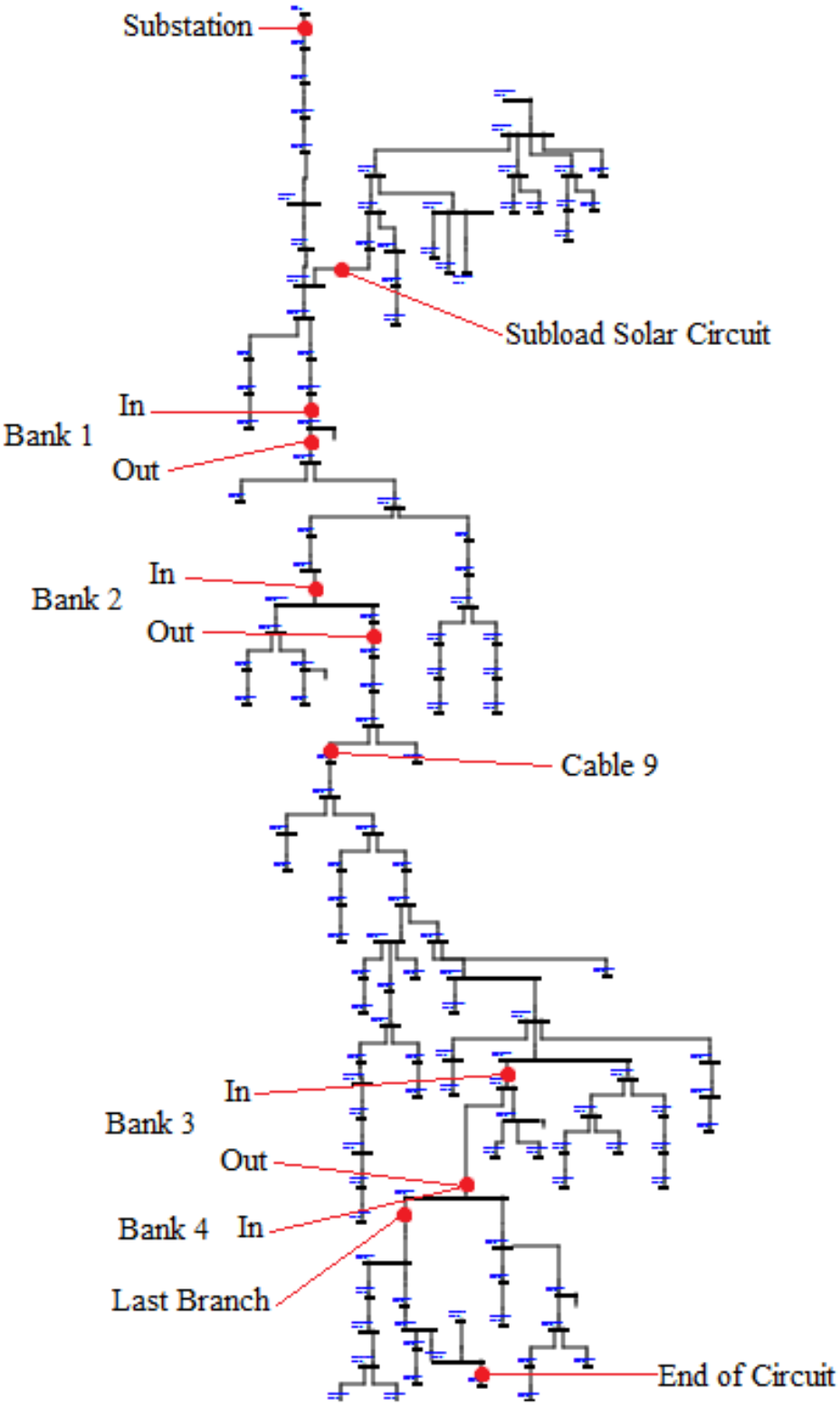

Figure 7: Measurement Points at SCE's Circuit

Simulation Results

Capacitor Banks		Substation			kVAR Flow in Points of Interest (kVAR)									Buses Information			Power Losses	
# of Active Banks	Active Banks	Active Power (kW)	Input Current (A)	Power Factor	Substation	Bank 1 Input	Bank 1 Output	Bank 2 Input	Bank 2 Output	Bank 3 Input	Bank 3/4 Out/In	Subload Solar Circ	Last Branch	Highest V (p.u.)	Lowest V (p.u.)	Undervoltage Buses	Active (kW)	Apparent (kVA)
0	None	6970	406	0.7972	5278.4	2621.9	2621.5	2382	2237.7	1053.1	766.4	1305.5	276.8	99.38	82.03	137 of 139	704	1520.76
1	1	6824	356.2	0.8886	3521.6	1184.1	2600.4	2361	2216.8	1050	763.8	1304.3	276	99.49	85.63	137 of 139	558	1143.40
	2	6824	356.2	0.8887	3521.1	1183.7	1183.4	944.2	2216.7	1050	763.8	1304.3	276	99.49	85.64	137 of 139	558	1143.40
	3	6801	356.1	0.8858	3562.2	1225	1224.8	985.6	841.4	-298	763.3	1304.3	275.8	99.49	86.35	137 of 139	535	1106.88
	4	6801	356	0.8858	3562.3	1225.1	1224.9	985.7	841.5	-297.8	-587.1	1304.3	275.8	99.49	86.37	137 of 139	535	1106.88
2	1, 2	6729	321	0.9715	1641.8	-493.2	1042.5	803.4	2195.4	1046.7	761	1302.9	275	99.6	89.43	137 of 139	463	896.77
	1, 3	6706	320.4	0.9700	1681	-451	1082.6	843.5	699.4	-423.2	760.4	1303	274.8	99.59	90.18	137 of 139	440	859.21
	1, 4	6706	320.4	0.9700	1680.9	-451	1082.7	843.6	699.5	-423.1	-712.2	1303	274.8	99.59	90.2	137 of 139	440	859.21
	2, 3	6706	320.4	0.9700	1680.2	-451.8	-451.8	-691	699.1	-423.5	760.4	1303	274.8	99.59	90.19	137 of 139	441	859.72
	2, 4	6706	320.4	0.9700	1680.1	-451.7	-451.8	-691	699.2	-423.4	-712.5	1303	274.8	99.59	90.21	137 of 139	440	859.21
	3, 4	6709	320.7	0.9695	1694.7	-438.7	-438.8	-678	-822.1	-1945.5	-739.1	1303	274.6	99.59	91	137 of 139	443	861.61
3	1, 2, 3	6674	309.4	0.9988	-324.6	-2405.2	-739.4	-978.5	543.8	-561.9	757.2	1301.5	273.8	99.71	94.25	69 of 139	409	770.51
	1, 2, 4	6674	309.4	0.9988	-324.8	-2405.2	-739.4	-978.5	543.8	-561.9	-850.9	1301.5	273.8	99.71	94.26	69 of 139	408	769.98
	1, 3, 4	6680	309.6	0.9989	-313.4	-2395.2	-730.3	-969.4	-1113.4	-2223.7	-880.1	1301.5	273.6	99.71	95.1	0 of 139	414	777.41
	2, 3, 4	6680	309.6	0.9989	-314.5	-2396.5	-2396.5	-2635.8	-1114.1	-2224.4	-880.4	1301.5	273.6	99.71	95.11	0 of 139	415	778.78
4	All Banks	6729	332	0.9384	-2476.8	-4675.8	-2864.4	-3103.7	-1435.4	-2532.7	-1036.6	1299.9	272.4	100.35	99.45	0 of 139	463	889.07

Table 3: Simulation Results with all Capacitor Banks possible cases

3.5 Results analysis

We can, first, classify our results in acceptable and unacceptable. Looking at the highlighted green lines, the only cases where all buses remain over 95% are with all capacitors, or with both 3 and 4 active besides either 1 or 2.

This alone tells us that the positioning of VAR Compensators influences in their system impact.

At our system, this can be explained by looking at the kVAR Flow at *Bank 2 Output* and *Bank 3 Input* in the cases of 3 active capacitors. In case both 1 and 2 are active, the reactive power flow is positive from Bank 2, feeding the circuit downwards. However, as they go through Cables 4, 6, 7 and 9, for over 8000 ft, the voltage drop is severe. This suggests that sending too much reactive power through this long distance is not good, promoting a high voltage drop; the power should instead come from the second part of the circuit. Cable 9 is represented on the system figure, showing the connection between two distant parts of the circuit as seen on Figure 2.

When we have, then, banks 3 and 4 active, which are on the bottom part, a negative reactive power flow is registered at *Bank 2 Output* (previously 543 kVAR, now -1113 kVAR), representing an oncoming reactive power from the below sub circuit, which then feeds the very same loads through the whole system, but from a different place. *Bank 3 Intput* also changes from -561 kVAR to -2223 kVAR, representing that what was only a parcel of a capacitor bank reactive power flowing back to the upper circuit, now is over one capacitor bank power.

As far as operational standards, most of the time it is desired that the system

operates as close as possible to 100% voltage on all buses, which means the ideal functioning scenario is with the 4 capacitor banks active at the same time.

Modifying this, however, might be of interest when taking into account a diversity of scenarios.

Graph 2 shows that we can actually reduce losses on our system whilst remaining in the operational 0.95 p.u. under voltage limit if correctly operating the banks. Therefore, for a given moment where we might have a generation fault or short, which reduces the system capacity to provide enough power, the system operator may choose to operate in special conditions.

Or even, if we would like to operate with a lower voltage – for instance, employing Conservation Voltage Reduction (CVR) in our transmission and/or distribution system.

The CVR technique has been discussed as one of the cheapest technologies that can ben intelligently employed to cut energy consumption [21]. Employing controls via Reactive Power Compensation, such as the capacitor banks discussed herein, can provide peak shaving, or cut energy consumption during abnormal scenarios in which demand surpasses limits [22].

Even though the results obtained from CVR vary from grid to grid, it is known that the savings do exist, for whichever load composition (between constant impedance, constant power or constant current) our grid may have [23]. Moreover, it is easy to realize from Graph 2 that not only the consumption can be controlled this way, but also the losses on our circuit may greatly benefit from using different voltage levels as set points.

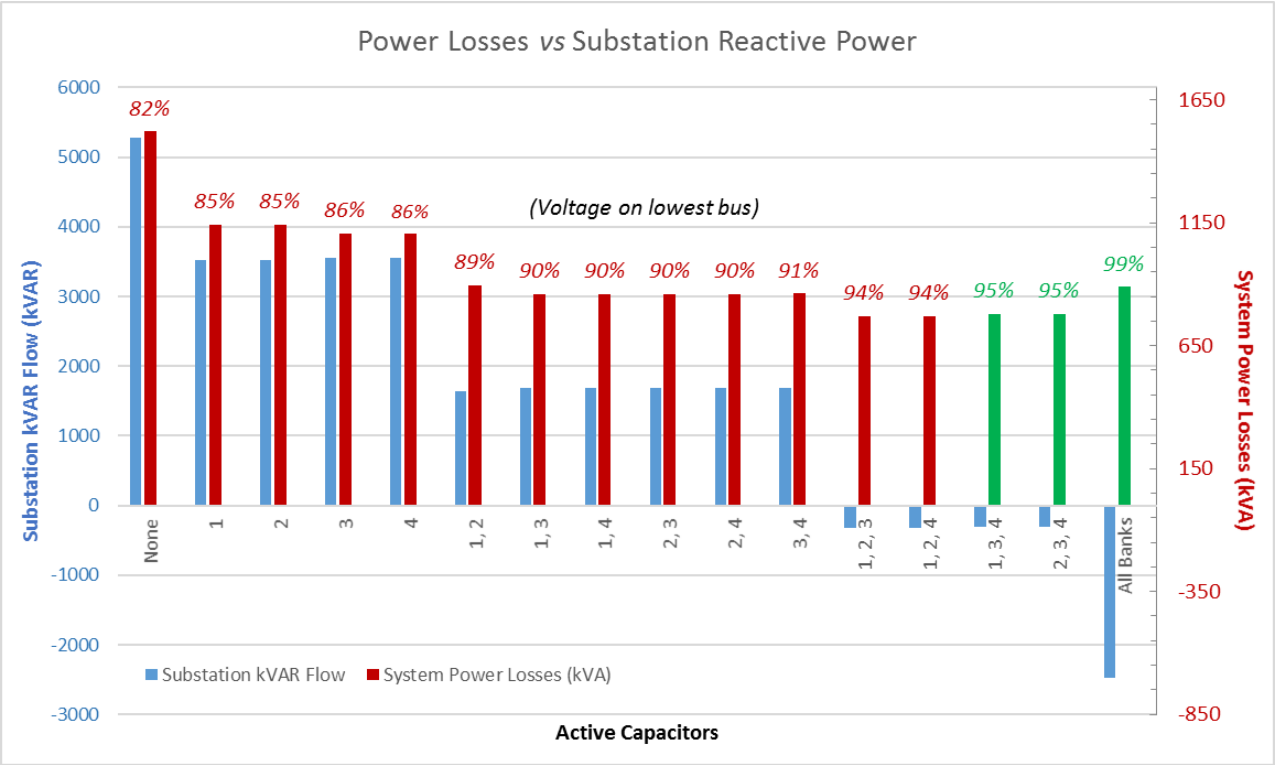

Graph 2: Power Losses Vs Substation Reactive Power, where the green bars represent valid operation points

Under these conditions, we must know beforehand how to properly operate between states. For our system, capacitors 3 and 4 play a vital role in maintaining the proper voltage levels at all buses.

At this moment, it is worth noticing that these effects regarding distance are different for different systems. This means that, in case we are dealing with a circuit of growing complexity, we may have growing complexity from different VAR Compensation positioning. Whichever the operators' intentions may be, whether it is desired to keep the voltage as close to 1 p.u. as possible, or if it is desired to reduce power consumption and losses momentarily, it is essential to understand the behavior of the grid on each of these states.

3.6 Summary of Findings

By studying the different arrangements in which the banks may operate at, we could identify the general operation method of the grid, understanding how the reactive power flow takes place in it.

Not only that, but we also have attested to the Chapter 2 theory development by confirming the need of local reactive power flow compensation to perform the proper voltage compensation; otherwise, the voltage profile falls below the allowable operational limits.

Furthermore, the location of each bank proved to matter when operating the system, which means not only does the VAR Compensation amount is meaningful, but also where it is allocated. By performing this analysis, we are now aware of which operational states are allowable and which are not, plus which are the most important capacitor for operation regarding losses and reactive power flow direction. Ultimately, VCR has been mentioned as an option to increase operation flexibility and diminishing losses.

Having this in mind, we can question whether the current positions of capacitor banks are, in fact, the best option possible. This questioning leads to further investigation and results in the Chapter 5 analysis, in which a method for optimal placement of capacitor banks is proposed.

4. TIME SEQUENCE SIMULATION AND ANALYSIS

A real transmission or distribution circuit has many changes in its load throughout the day. During night, there is a smaller load demand, whereas during day most industrial and residential loads are consuming power. Every time we switch an electrical equipment connected to the grid, we are changing its loading, and the aggregate of all consumers' loads turning on and off compose a load profile. Therefore, not only electrical systems have different load conditions, but also conditions varying through time.

A load profile curve enacts this behavior, and by studying the system under these conditions, we are able to properly represent the real grid functioning. Moreover, this allows the anticipation of the power demand [24], which is of great interest to utilities, even more so if we increase our renewable penetration on the grid [25], when the complexity of operation is increased.

4.1. Simulation Circuit

SCE's circuit, as every other distribution circuit, has a Load Profile which shows how does power demand varies within time. For our circuit, we will use a daily load profile which was measured in the very own circuit simulated. The measurements took place on a Friday, in which power consumption levels are similar for other working days – and higher than weekends and holidays. The load profile curve can be seen on Graph 4.

Early hours have very low consumption, and the load gradually increases until a maximum of over 7 MW, around 5 pm. As it was a Summer day, we will take this as the circuit nominal load, since the peak demand is registered during summer for that region

[26].

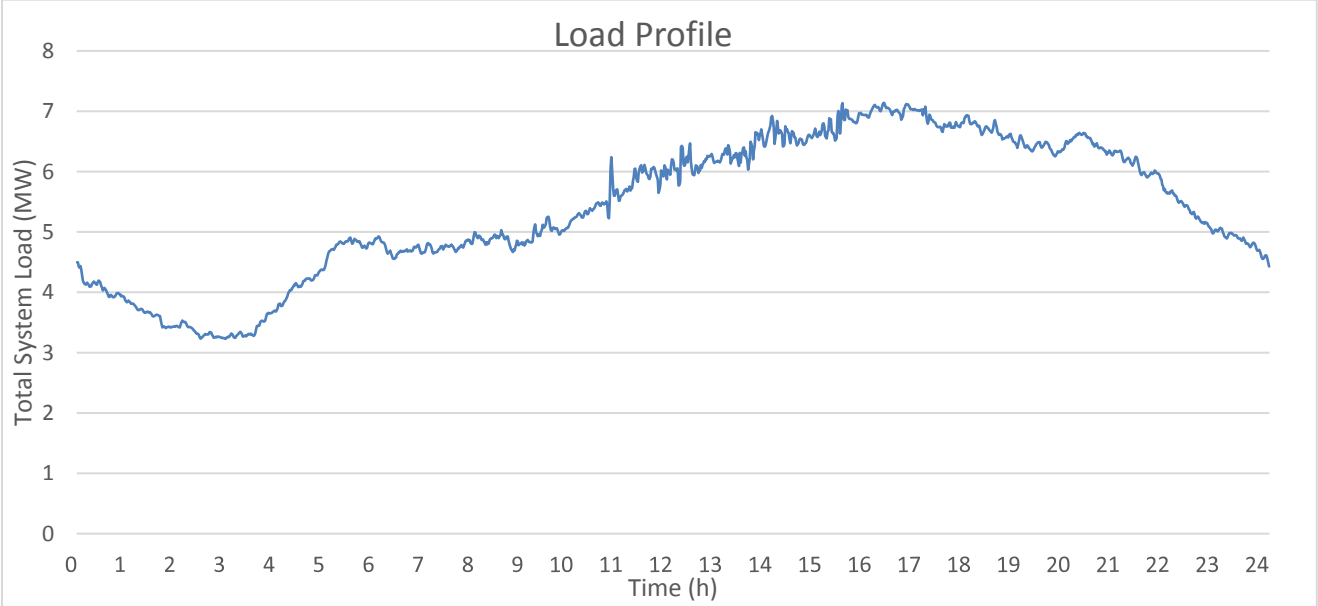

Graph 3: Load Profile from SCE's circuit

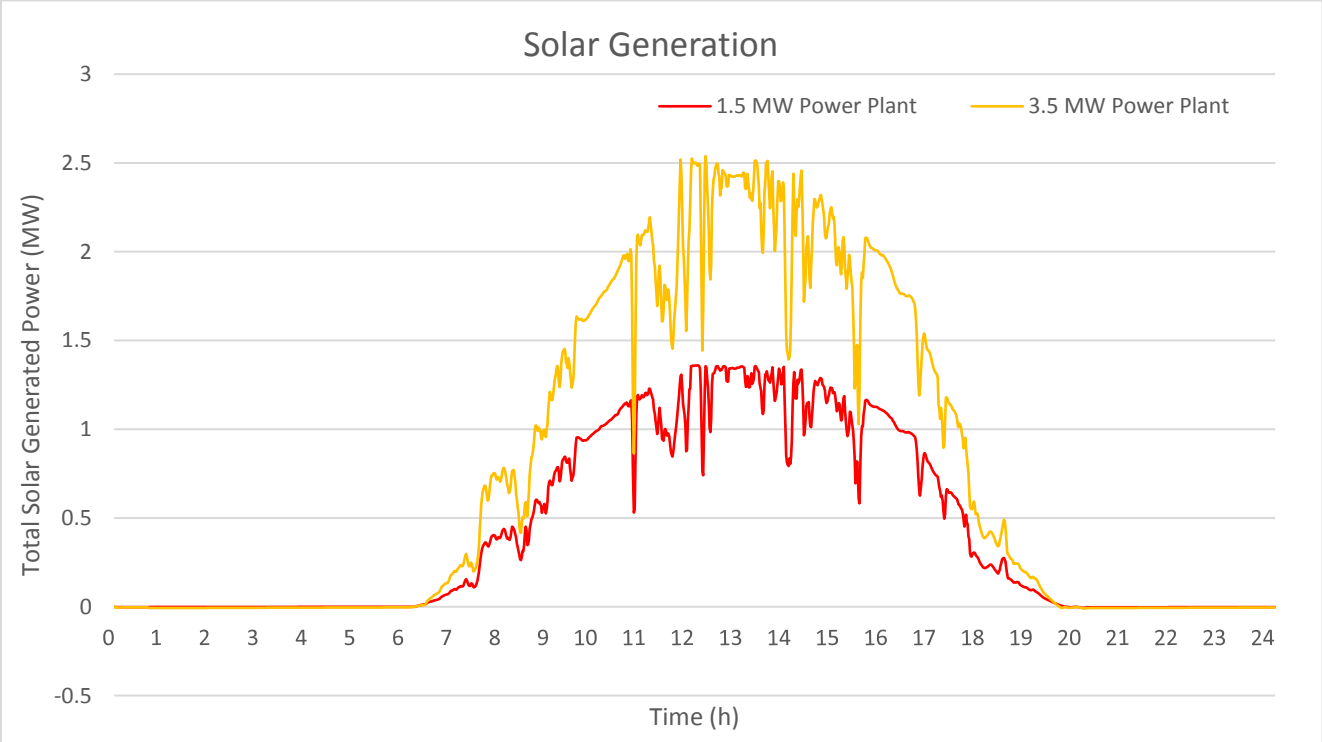

Graph 4: 1.5 and 3.5MW Solar Plants Generation Profile

Additionally, we will utilize two additional curves representing the power generation from each of the two solar plants, shown on Graph 5. These also depicts actual measurements from the grid, on the same day of the load profile. The day in question is an August day, and having that the circuit is present in California, we can relate the solar generation with a solar irradiance curve. It is also worth noting that the differences between the generation curves are related to the arrangement of the solar panels, such as angle positioning and other factors, besides their different nominal powers.

The difference between the power demand and the solar generation is shown on Graph 6.

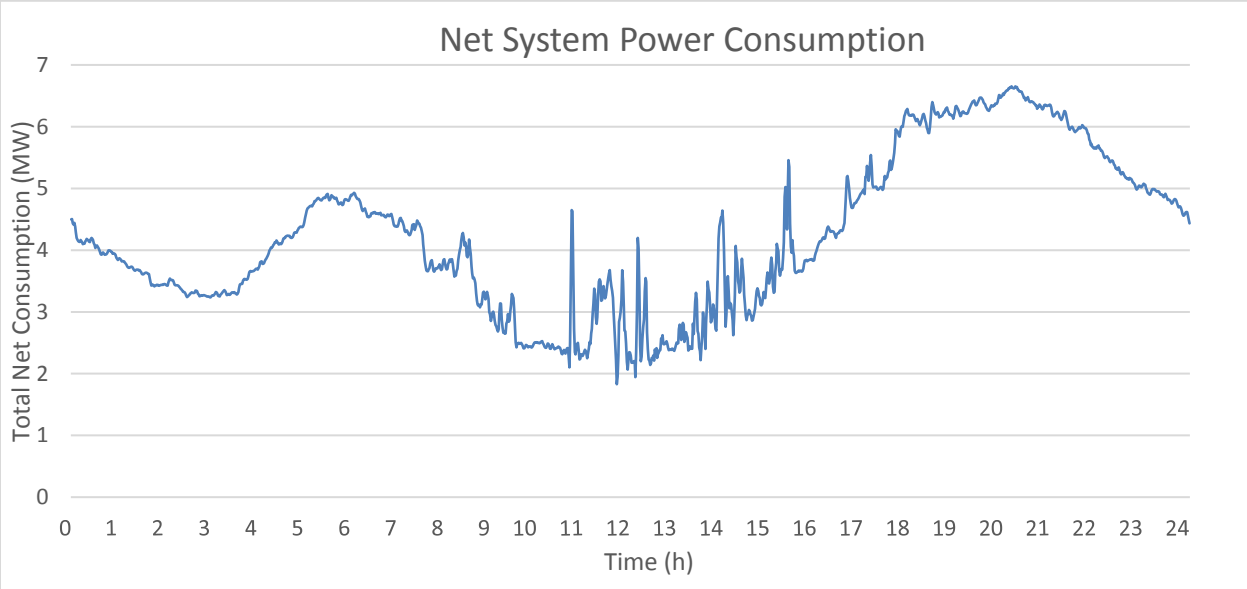

Graph 5: Net System Power Consumption

In daily operation, the activation of the Capacitor Banks must be made by trigger voltage levels in the buses. We cannot have a fixed operation, since it changes accordingly to Graph 3.

These levels have to be designed according to the system's specifications, so that there will not be any possibility of "non-operating zones" nor "super-excited zones"; for instance, in which the capacitor bank would uninterruptedly trigger on and off.

We can set, for example, the capacitor voltage levels to act activating at voltage levels below 0.98 pu, and disconnecting at 1.02 pu. We can see that, at both extremes of operation, at 30% and 70% Loading cases, these capacitor triggering levels would be situated in stable regions.

From Graph 6, if we have 30% loading and no capacitor active, it would fall below 0.98 pu, thus turning one capacitor bank on. This would raise the voltage profile globally, above 0.98 pu.

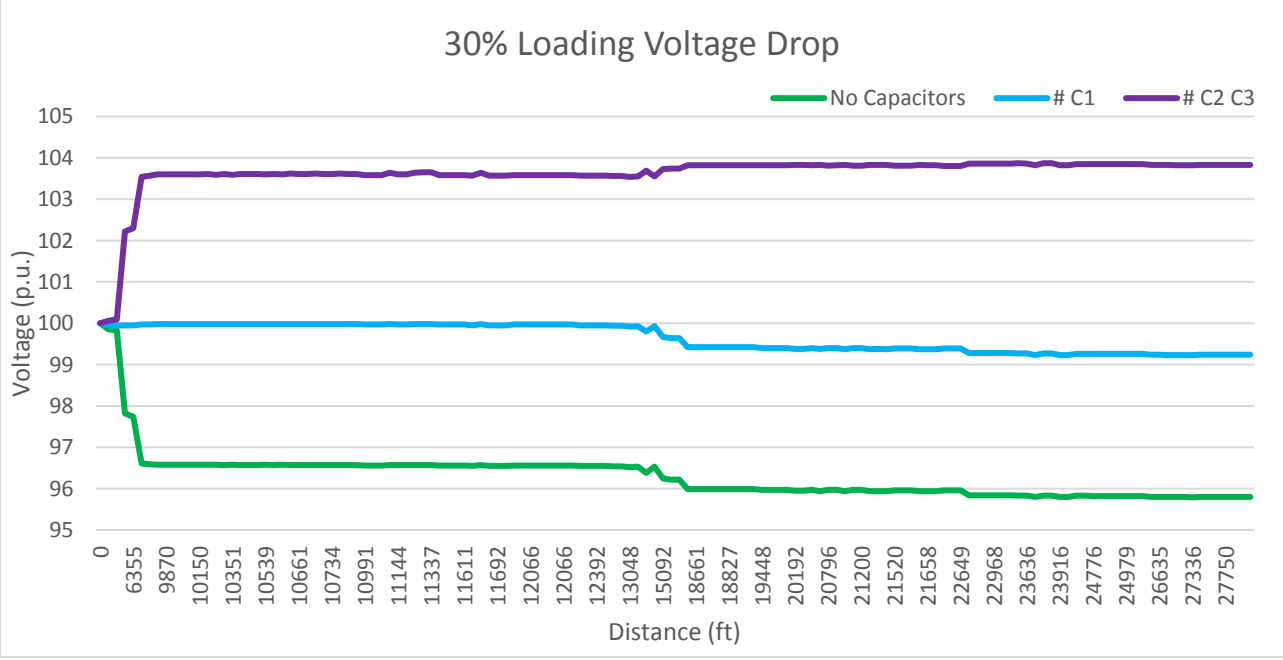

Graph 6: Voltage Drop with 0, 1 and 2 banks, under 30% nominal load

In case our load increases to the upper limit, at 70%, the same applies: at first, up to three capacitors would be triggered on, as after each, the voltage would still be below 0.99 pu. Once the third capacitor is activated, the voltage profile rises above 0.99 pu, but below 1.02 p.u.

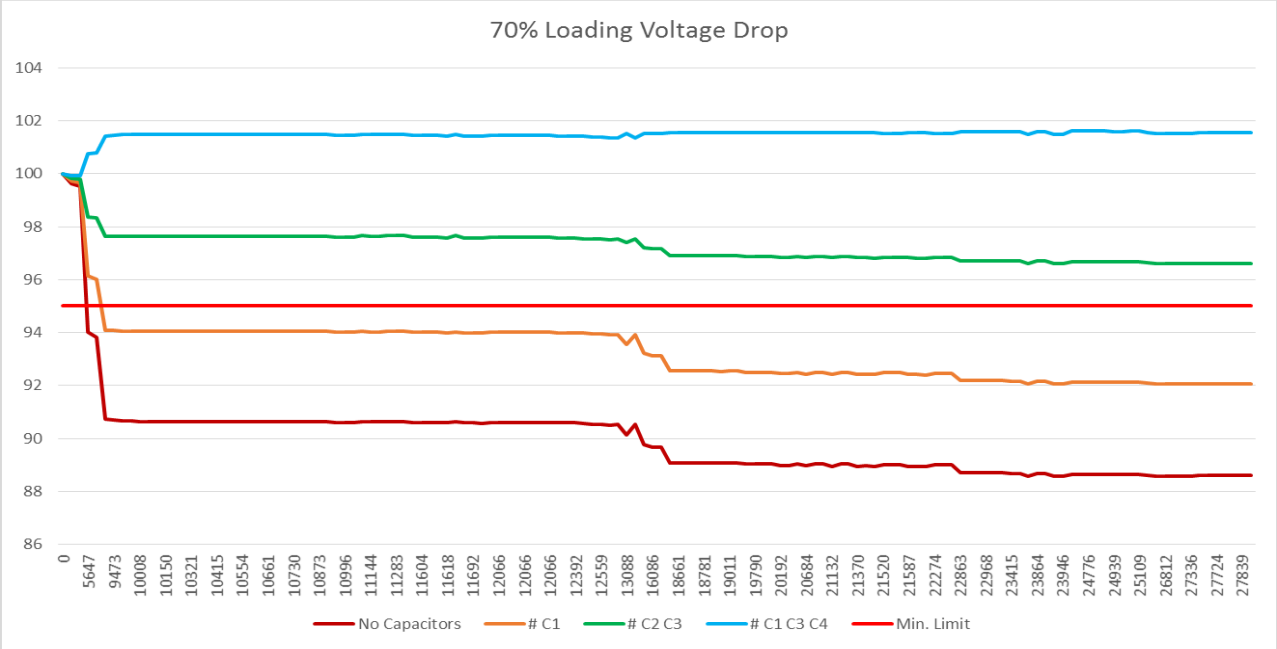

Graph 7: Voltage Drop with different banks active, under 70% nominal load

However, these values must also be so that switching operation throughout the day, according to the load profile Graph 3, is not excessive nor flawed. To test it, we perform a load flow through time, considering these values and variations.

4.2 Software Simulation Tool

At this moment, we will switch our simulation tool and use OpenDSS 7.6.5.18 to perform the simulations. This software utilizes a command window instead of a Graphical User Interface. We can see some of the code lines exemplified at Appendix I, where it is included the declaration of electrical lines.

Note that most graphs depicted here will display phase values, instead of total values. That is valid for active and reactive power graphs, which have three different colors corresponding to each different phase. The simple sum of those values will add up to the total, three-phase value. Also, the x-axis is shown at seconds, on a total of 86400 seconds comprising one full day.

When initially simulating the circuit at OpenDSS, we still do not enable the distributed generation. Once we ensure our circuit is properly functioning, we can proceed to the next step.

As there are no other active power generation within the circuit, we expect to see a curve which follows the circuit load profile, in Graph 3. We can see from Graph 8 that it, indeed, follows the expected behavior, and the sum of the three phases active powers represents the load demand.

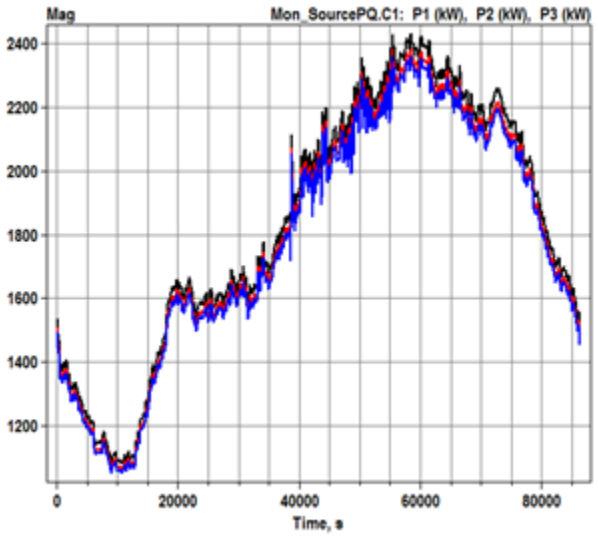

Graph 8: Substation Active Power Flow through time

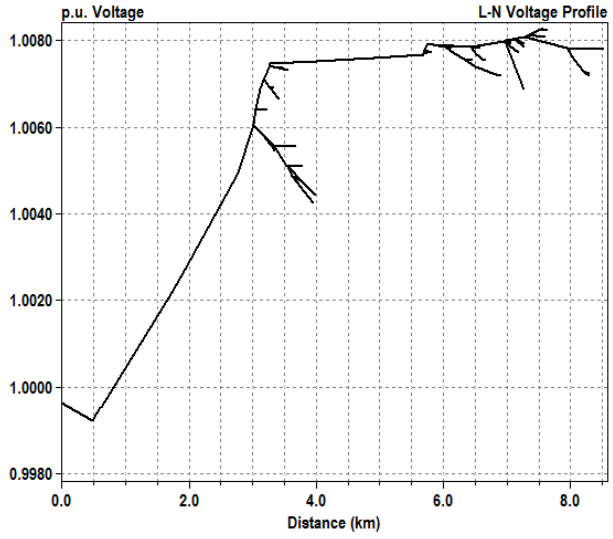

Graph 9: Voltage Profile across circuit at last instant

Also, Graph 9 represents the voltage profile of phase A at the last moment of the simulation. It stays well within the 0.95 to 1.05 p.u. stablished limits.

4.3 Load Profile and Solar Distributed Generation

Next, we are going to include the solar power plants of 1.5 MW and 3.5 MW, according to Graph 4.

4.3.1 Non-coordinated Capacitor Banks

At an initial moment, we use desired settings without much consideration for the previously simulated circuits. That means we arbitrarily choose triggering points for each capacitor triggering.

In case we select 0.99 and 1.01 pu as lower and upper limits for turning each capacitor bank on and off, respectively, we obtain the following result for banks #2 and #3:

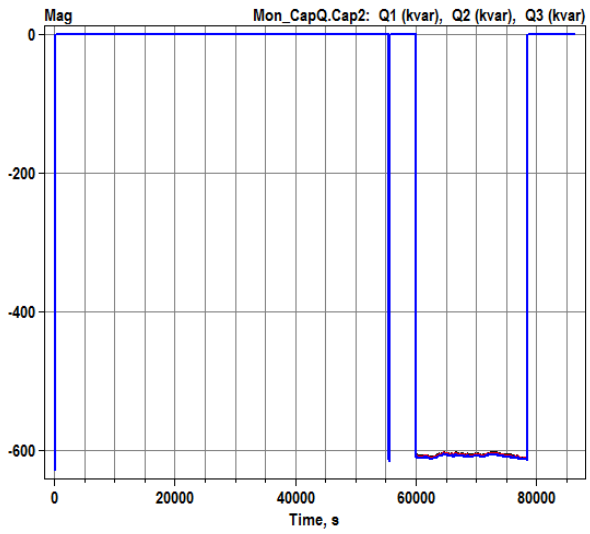

Graph 10: Uncoordinated Capacitor Bank 2 Activation

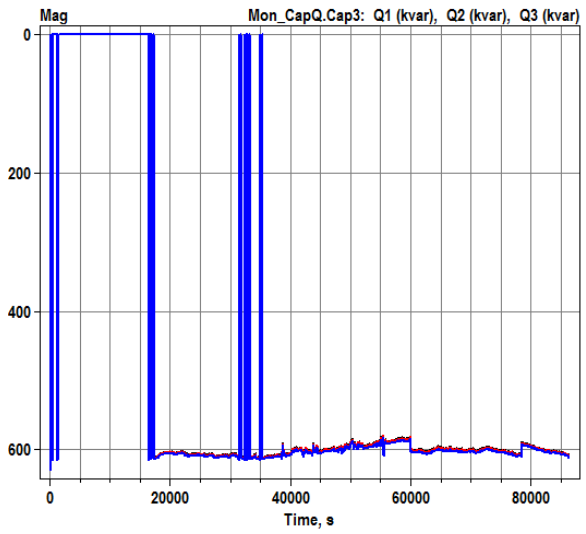

Graph 11: Uncoordinated Capacitor Bank 3 Activation

It is clear the undesired excessive switching of capacitor banks #2 and #3. At the first few minutes, again at 300 minutes, and yet again at 540 minutes, the bank is constantly triggered on and off. Even though all banks are set with a 1-minute hysteresis time, and with a deadzone of 5 minutes, this does not stop the capacitor from constantly switching.

Every time it operates, it provides over 600kVAR to the grid, whose voltage then reaches values higher than the capacitor upper level triggering limit, and the same for its off state. As, at the same moment, the load is varying and also the solar generation is having intermittency effects, the capacitor control fails to properly operate it.

The downside of this operation as is, is the rapid wearing off from the excessive and frequent mechanical triggering, besides provoking instability in the grid and bringing an unstable condition. We must, therefore, change the circuit settings for proper functioning.

In case we increase the deadzone and hysteresis time, the response of the system will be too slow, and may compromise normal operation status, not to mention emergency operation status. Therefore, to better handle this situation, we will take into account the analysis developed previously, and select suitable triggering levels for our circuit to work as intended, taking into account the penetration of the solar power into the grid and its possible intermittency problems.

4.3.2 Coordinated Capacitor Banks

If we get back to Section 4.1, when moderate and low system loadings took place, we can see good operational standards fall within 0.98 and 1.02 p.u. Once we change all capacitors switching points to those values instead of arbitrary desired points, we have a smooth operation. That is depicted on the next set of graphs.

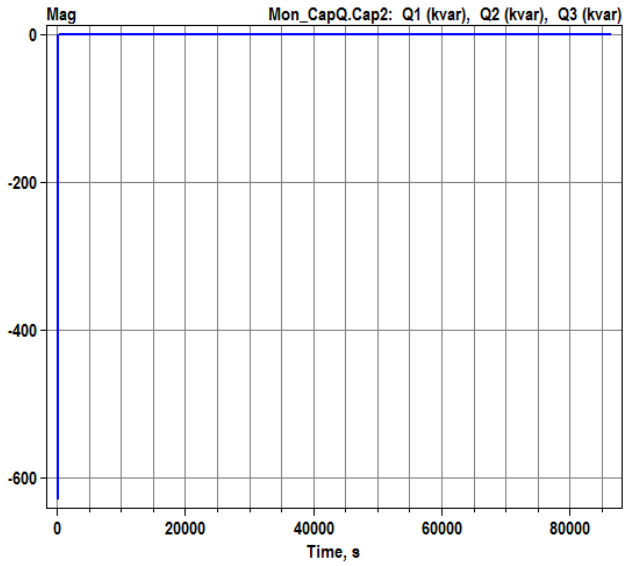

Graph 12: Coordinated Capacitor Bank 2 Activation

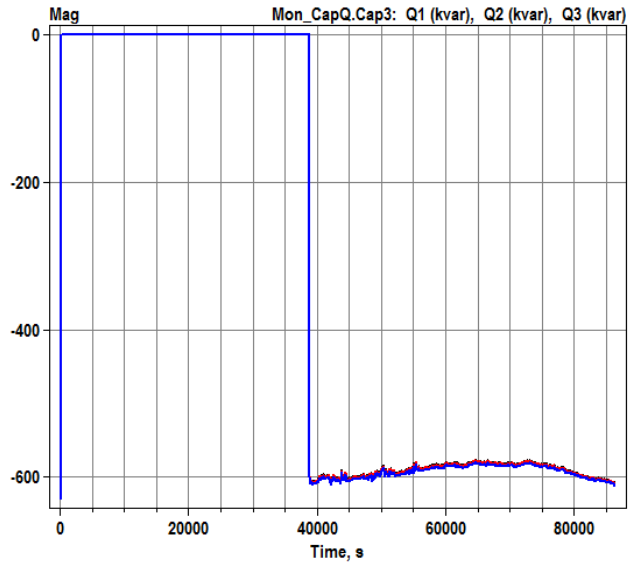

Graph 13: Coordinated Capacitor Bank 3 Activation

Now, we no longer have the undesired excessive switching from the capacitors. However, Capacitor Bank 2 is not triggered at all, not even when a high load is present. That means we will have lower voltages across the system, which might be undesired. For instance, at the end of circuit, we have close to 0.98 p.u.

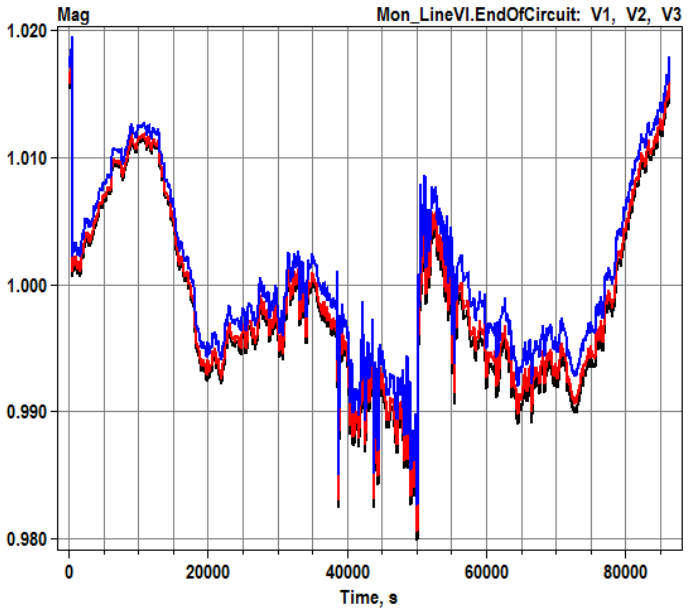

Graph 14: End of Circuit voltage

To fully study the effect of all capacitors on our system, we will change slightly the triggering settings, so that our system will go through activating all capacitor banks. The capacitor settings are, then, set to 0.99 and 1.02 p.u. to banks #1 and #4, and 0.985 and 1.02 p.u. for banks #2 and #3. These decisions are based on the results depicted on Table 3, agreeing that the latter should have priority in its activation versus bank #2.

4.4 Simulation Results

Let us initially look at banks 2 and 3, and compare to the previous results.

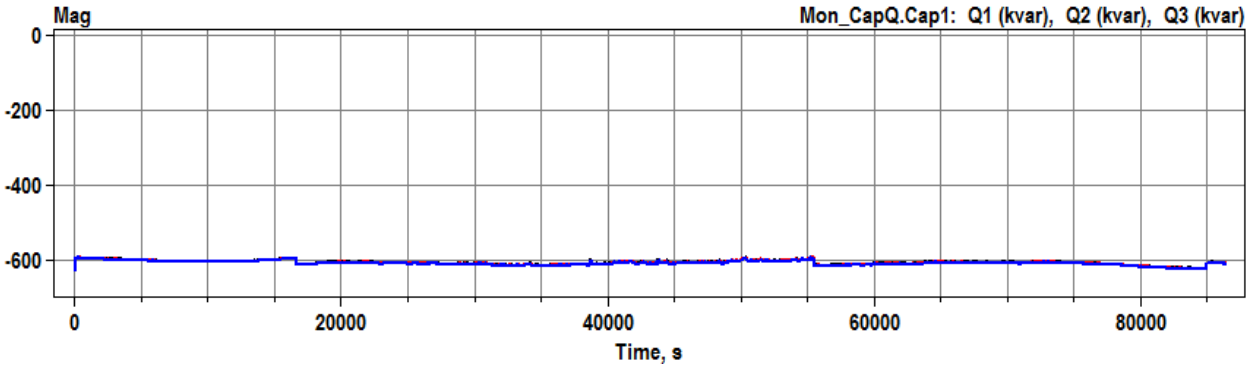

Graph 15: Capacitor Bank 1 Activation

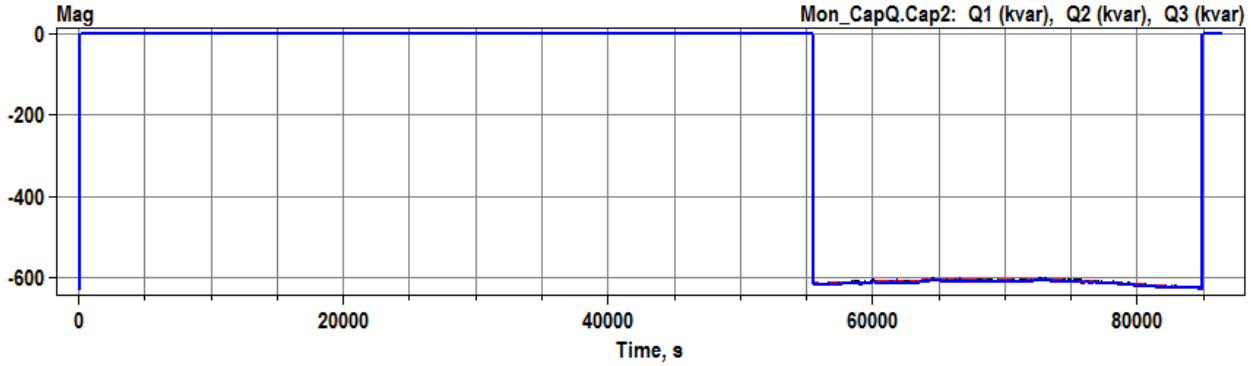

Graph 16: Capacitor Bank 2 Activation

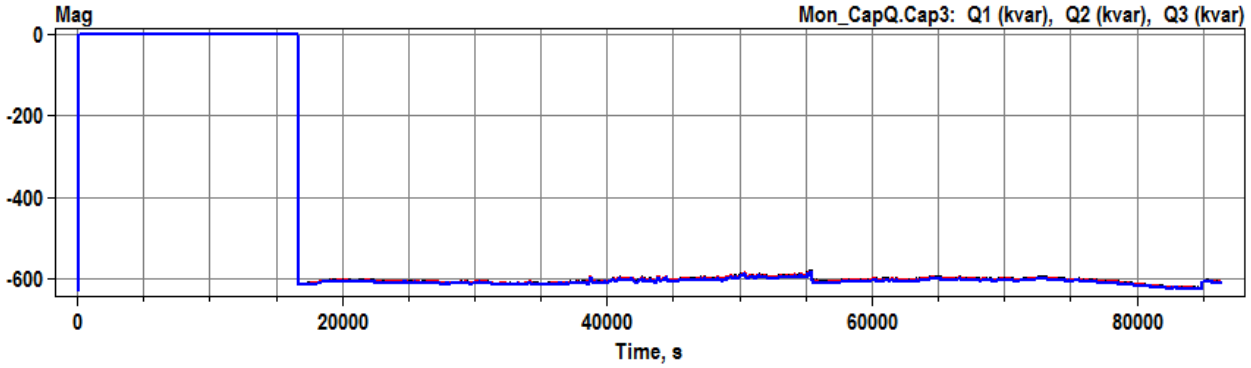

Graph 17: Capacitor Bank 3 Activation

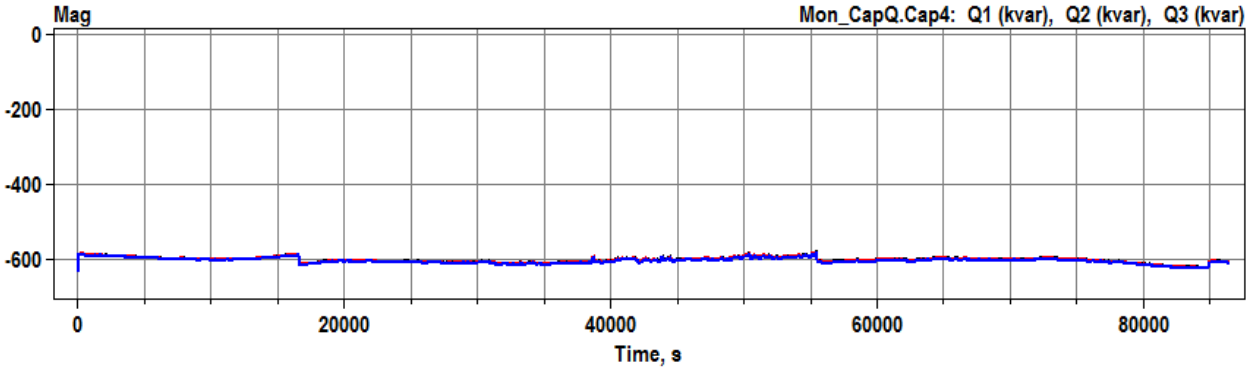

Graph 18: Capacitor Bank 4 Activation

We can see Capacitor Banks #3 switches first, given it has a lower voltage across its regulating bus. This actually agrees with the results obtained from 3, where we established that capacitor 3 and 4 should have priority over capacitors 2 and 1, respectively.

Also, bank #2 activates when high demand is in effect, accordingly to graph 3, without any frequent switching effect. Next, we can observe the power from banks 1 and 4, which are always on, on our given settings.

It is possible to see that, whenever another bank is triggered on, we have a slight increase on the reactive power for other banks already on. That is due to the increase of the voltage across the system once we have more reactive power; and by having a higher voltage at their buses, the capacitor, modeled as a constant impedance, will have its current increased once we increase the voltage across it. This results in more power, as a result of the multiplication between current and voltage, both higher.

Additionally, comparing to Graph 6, we see that even under low load, we are required to maintain some banks connected. This agrees with results from Graphs 15 and 18, where the capacitors were not disconnected at any moment by our control strategy.

Next, we will observe the substation active and reactive power, per phase.

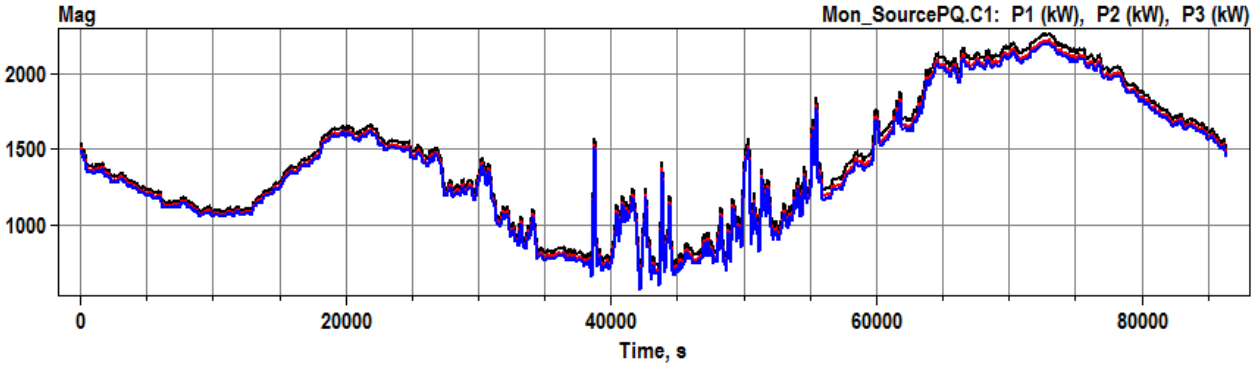

Graph 19: Substation Active Power Flow

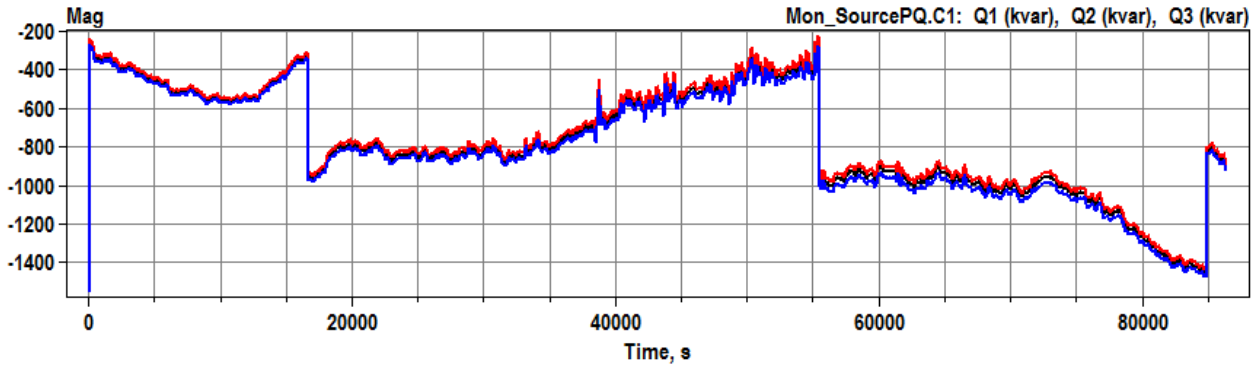

Graph 20: Substation Reactive Power Flow

By looking at Graph 20, we have results that agree with that developed at Section 3. The power flow is negative towards the substation, which means it is absorbing reactive power from the grid, in order to keep the voltage level across the system as close to 1 p.u. as possible. Also, we can note each capacitor switching taking place, whenever there is a rapid alteration to the substations' reactive power, during activation of banks 3 and 2, and deactivation of bank 2, respectively.

Regarding the active power, we can clearly see the effect of the solar power plant, depicted on Graph 4. The substation has to provide less and less active power as the sunlight bathes the solar farms, but provides a backup in case there are interruptions due to weather intermittency. As the day reaches its end, the solar farms are able to provide less power, in which moment the substation takes over the power supply, up to 6800 kW in total. In

comparison with Graph 8, we see a relevant difference, and over the day, there is considerably less need for the substation to provide active power. This reduces proportionally the grid losses, since the current going through the feeders is smaller.

Also, we can observe the end of line voltage. It remains within our established limits of 0.99 – 1.02 p.u., all well within the tolerance margins of 0.95 to 1.05 p.u.

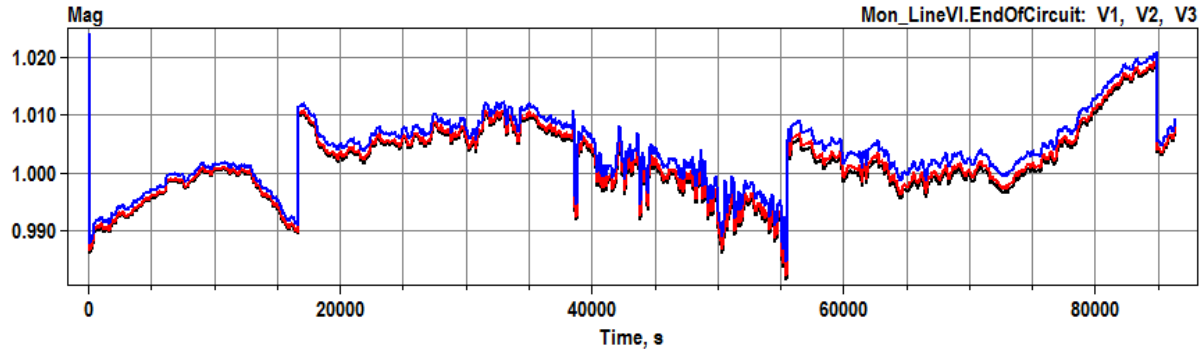

Graph 21: Voltage at End of Circuit

Finally, we can observe the voltage profile of phase A across our circuit. Graph 22 shows the profile at noon. We can observe there is a voltage drop throughout the initial transmission lines, where the voltage dips below 1.0, and increase as we go further into the circuit, where capacitor banks are present. Then, as is goes over 7 km, it decreases below 1 p.u., but stays within a very close range.

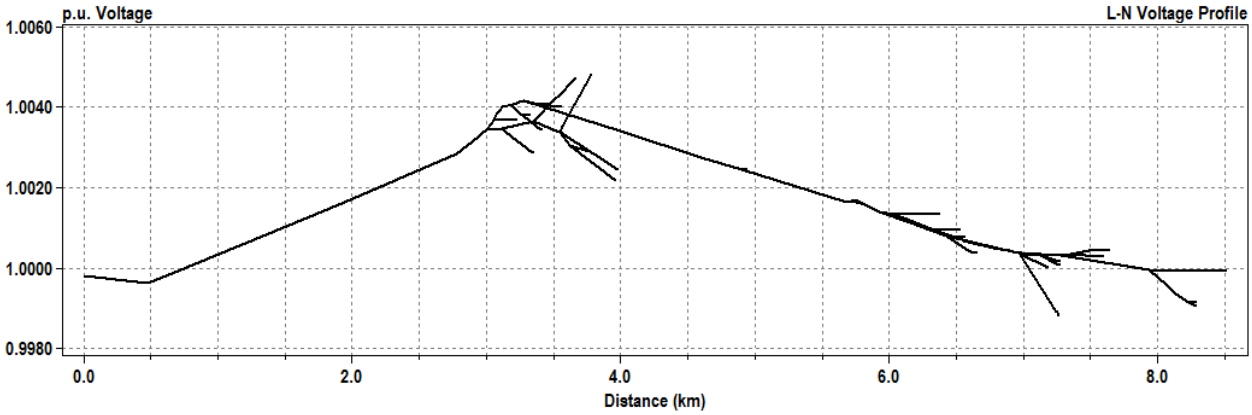

Graph 22: Voltage Profile Across Circuit at Noon

4.5 Summary of Findings

By utilization of renewables, when comparing Graphs 23 and 24, we can clearly see the difference between the substation current towards the circuit in presence and without the solar power plants. The circuit losses, proportional to the square of current, are therefore largely alleviated.

In addition to that, there is more of the transmission circuit beyond the substation, not analyzed in this thesis. The additional distance between generator and our distribution circuit is not accounted for; however, in reality it is, wherever that power flow takes place. The distance through which the current travels in reality is much longer, and the amount of losses are proportionally higher.

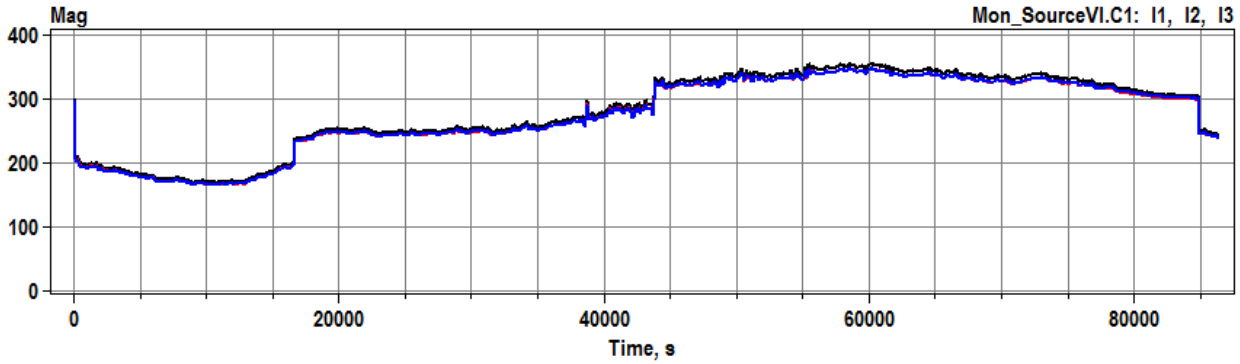

Graph 23: Substation Current without Solar Generation

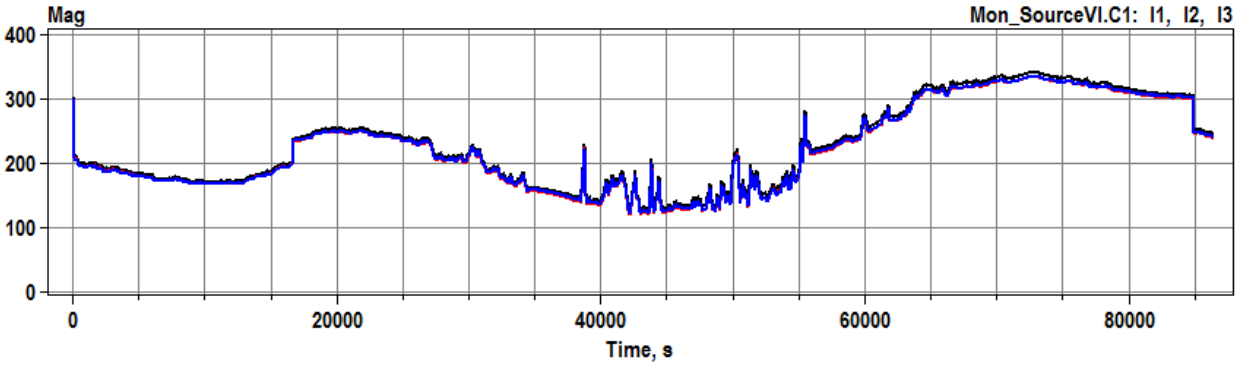

Graph 24: Substation Current with Solar Generation

This means not only our grid is using renewable energy, but also achieving a much higher efficiency doing so, avoiding long transmission lines and cables, promoting less displacement of the energy involved.

In this section, we analyzed how well we can cope with grid standards under influence of high penetration of distributed renewables generation, using capacitor banks as our only VAR Compensation method.

Taking the knowledge developed in the last two chapters, a new technique is developed and analyzed, implemented and simulated on this very circuit, throughout employing the same techniques in addition to a visual aid analysis.

5. OPTIMAL CAPACITOR PLACEMENT AND SIZING FOR LOSS REDUCTION USING GRAPHICAL TOOLS AND POWER FLOW OPTIMIZATION

As we have seen, the placement of capacitor banks does interfere with the functioning of the circuit; moreover, their size also affects the overall functioning of the circuit.

Therefore, by improving the efficiency of distribution system through optimal allocation of capacitor banks, we can achieve a better efficiency of the overall system [27].

When designing or studying a system, we can make use of diverse tools to make that objective feasible. The placement and sizing of capacitors is one important aspect that, if improper, can lead to negative results, or even forbidden operational states. There are many techniques to optimize the distribution of reactive power compensation technologies inside the grid; however, most of the available material involves different techniques and theories which lack simplicity for general implementation [28 - 35]. The lack of a visual approach, using the information of distances as well as loads in a quick fashion is noticeable.

With this, there is motivation to perform a more direct approach, rapidly adaptable to other systems, and with simplicity for its easy implementation. The desired effect is to ensure small losses whilst making possible the operation throughout the day. In addition to that, this technique encompass integration with high penetration of renewable power generation. Besides that, coordination is achieved by ensuring proper operation levels, and counting with a reduced switching frequency.

5.1 Method Description

The proposed guidelines for optimal placement and sizing of capacitor banks are going to be discussed in this section.

First, with aid of visual tools, the spatial distribution of the loads is considered for the task of capacitor placement. Next, the power flow of the system is performed and, with thorough analysis, the optimal sizing of each capacitor bank is achieved. Finally, the switching coordination is achieved through studies with the load profile time-simulation analysis.

During the explanation of this method, all steps will be applied to SCE's circuit, so to compare and verify the method - having in mind its present functioning shown on Chapters 3 and 4.

The summary of the steps can be seen below, arranged in three groups.

1) Capacitor Placement (Graphic Analysis)
- i) Physical Distance Mapping
- ii) Load Visualization
- iii) Capacitor Placement

2) Capacitor Sizing (Power Flow Simulation)
- iv) Reactive Power Determination
- v) Capacitor Sizing

3) Switching Coordination (Time Sequence Analysis)

5.1.1 Capacitor Placement

i) Physical Distance Mapping:

A physical distance mapping is done with the information of the desired grid. In case there is no drawing available, aid of tools such as MATLAB software is needed. In this work, the whole procedure was done extracting the distances information and inputting it to MATLAB. This initial step can be seen on Appendix II.

ii) Load Visualization:

Next, a load mapping is performed, adding information to the initial map.

All loads must be represented on their actual sites, and on proper scale to suit the map size. In order to handle different variation between the loads of a same circuit, another factor is included exponentially. The resulting formula for representation of each load on the map drawn on i) is given by:

$$S_{size} = K.S^{\alpha} \quad (5)$$

Where:
S: Load size. Its unit (VA, kVA, MVA…) must be consistent for all calculations;
α: Exponential factor;
K: Linear factor, chosen so to make the visualization clear (ft/VA, ft/kVA, m/VA, m/k, etc, according to the previously used units and designed map);
S_{size}: Resulting radius size for the circular representation onto mapping (ft or m).

The value for α is taken according to the variation between loads. For instance, visualizing loads in the range of hundreds of kVA and small kVA in the same map would not be possible, since there is a scale factor of over a hundred between these set of loads. To overcome this limitation, the exponential factor is implemented.

The value for α is given by Graph 25. Different proportions will render different values for α, and the Scale mentioned from this point on (x10, x25, x50) regards the proportion between the maximum and minimum S_{size} values, whereas the Load Proportion regards the proportion between the maximum and minimum values for each load, S, initially given.

If wished, it is possible to take this adjustment as a linear scale and maintain α = 1. However, here we will follow the procedure and proceed with a x25 scale, so to better visualize the whole spectrum of loads. Our load set has a proportion between its maximum and minimum values of 2700, and therefore we choose α = 0.41.

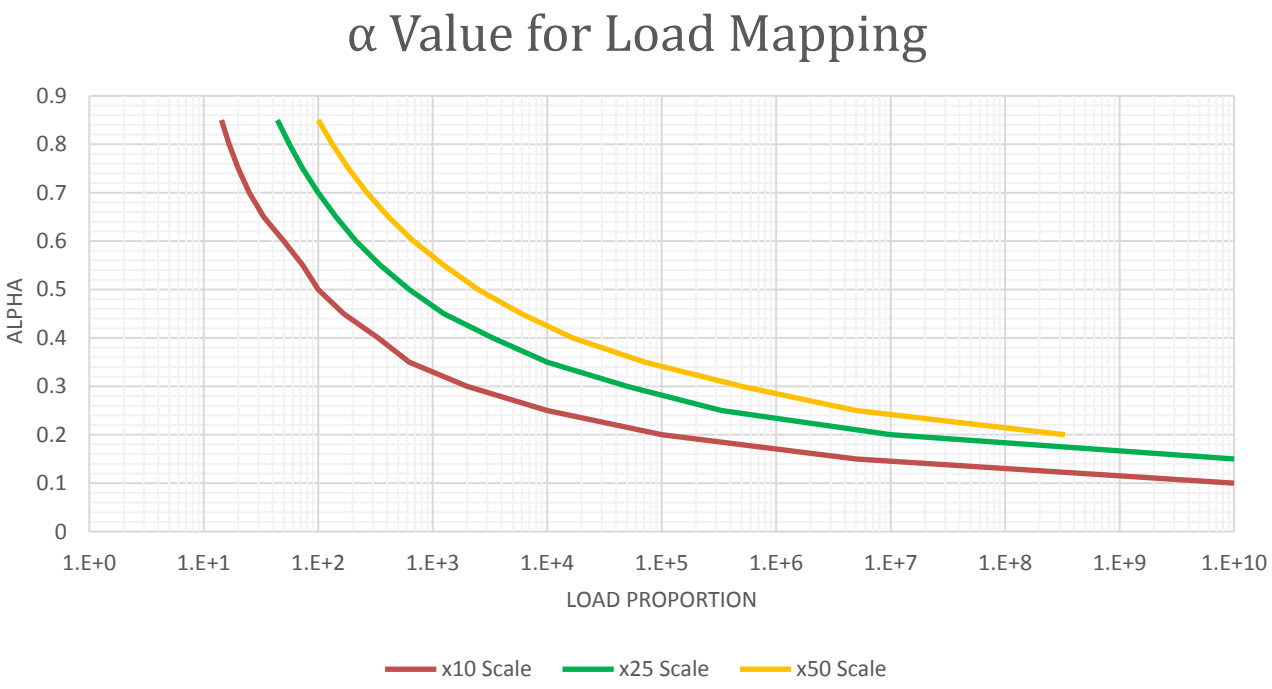

Graph 25: α Value for Load Mapping

Next, K is used to improve visualization. Different values can be tested to determine which K will enhance the image at its the best. A suggested range of values is using Formula

6, where k ϵ [0,1) may be chosen at the user's discretion. It is, however, recommended to pick 0.15 ≤ k ≤ 0.25.

$$K = \frac{min\,(y_{range}, x_{range}).k}{\max(S^{\alpha})} \quad (6)$$

Where $\min(y_{range}, x_{range})$ is the minimum value between the *x* and *y* axes' ranges.

Executing the Load Mapping procedure with α = 0.41 and k = 0.22, we get Figure 8 as a result. When comparing to the linear scale plotting available on Appendix III, which shows directly the values of S, before using formula 5, we can see how much more information is presented on this graph. Additionally, Appendix III also shows different cases with varying values for α and k.

Lastly, it is worth noticing that, in case the load group has, for instance, only one very small load within a much larger and numerous group of other loads, it may be useful to disregard that specific load within other calculations.

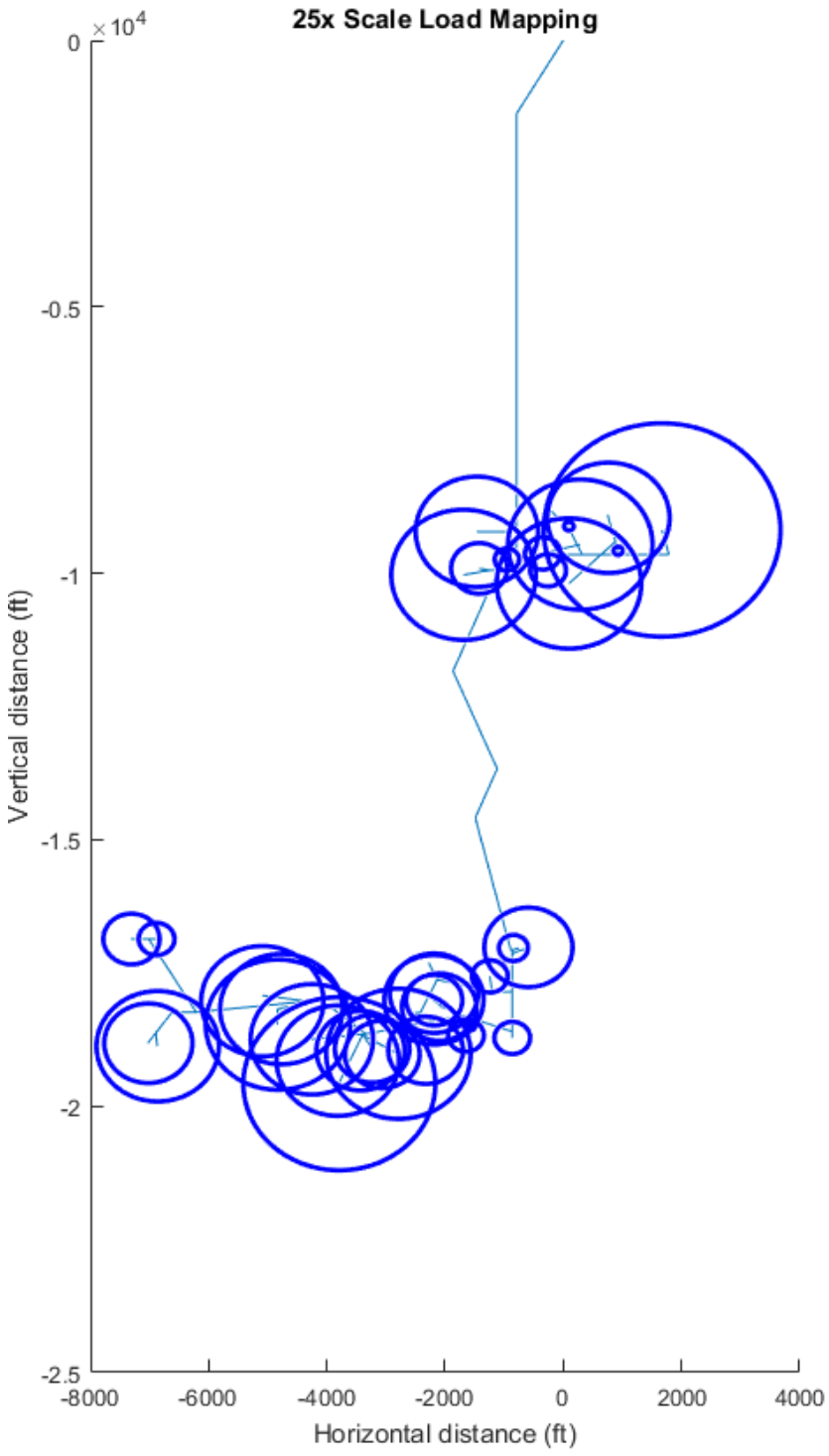

Figure 8: Load Mapping with x25 scale, on top of Physical Distance map

iii) Capacitor Placement

Area distinction: According to the resulting image, different areas are set within the map. At Figure 8, we can see two distinct areas separated. They are, then, named A_1 and A_2, where the second is the bottom area. In case the load mapping presents more than two areas, they may be separated according to the resulting image from the previous step.

Number of banks: as we have a varying load, according to Graph 4, we need at least two capacitors on the whole system to switch between operational states, otherwise we will have overvoltage or under voltage should only one capacitor be used, as seen on Chapter 3. In addition to that, we wish to minimize the losses, which means ideally each area A_1, A_2, … A_n, would have most of its reactive power demand locally supplied, using nearby capacitor banks.

Additionally, in case we have only one capacitor per area, the reactive power flow in the long cables will reach high levels, as we have witnessed on Chapter 3 analysis, taking that our areas have similar loading levels – visually confirmed. To secure a better system efficiency, therefore, we need at least a pair of capacitors in each area, so that intermediate loading levels have at least some reactive power locally supplied, instead of requiring a long travel from kVAR.

Moreover, the more capacitors we have on the grid, the less losses we will have overall. This is due to having a closer match from the required kVAR to that one provided. However, the more capacitors we have, the more switching operations will be present on our grid, which is a limiting factor.

Therefore, we need to cope with the maximum allowable daily switching operation

number (MADSON) [35] of the grid, and select a number of capacitors between the minimum necessary and maximum allowed.

To achieve this maximum number of banks, we take into account the maximum load variation from the day with the most changes in the voltage profile, such as the peak summer consumption, and calculate the percentage of variation (S_{change}) in respect to the peak hour load. For instance, if at an industry the day starts with 0 kVA consumption and grows up to 10 kVA, it would have 100% variation; if, instead, it raises from 1.5 to 10 kVA in the peak day, this would represent an 85% variation.

With this definition, we can apply the following:

$$Max. Number\ of\ Capacitor\ banks = \frac{MADSON}{2 * S_{change}} \quad (7)$$

Another factor to take into account when choosing the number of capacitors is the decreasing value of kVAR compensation as the bank size increases. The more capacitor cans, more stainless steel is required for the cans, more bushings, more welding, more labor, higher shipping costs; as for the racks, complication and size increases with more cans and thus price goes up the more we segment our capacitors. That means 8 banks of 900 kVAR would be more expensive than 4 banks of 1800 kVAR.

That means choosing a number will have to take into account:

- Decreasing losses with more capacitors;
- Increasing switching stresses with more capacitors;
- Increasing costs with more capacitors;
- Market availability of capacitor values.

The gains in term of decreasing losses with more capacitors are, however, remarkably small. Additionally, one could try and maintain the number of banks at an even

number, in case there is an even number of areas, so to better balance the grid operation.

When reviewing or designing a system, a trade-off has to be taken into account. In this thesis, the following work is based on the assumption of less acquisition and installation costs.

Another important reminder is that restraints must be studied according to the load profile and load flow characteristics of the used circuit. Additionally, if a disproportional A_3 very small is present, for instance, then only one capacitor bank is implemented at that area; if an area A_4 has more than twice the amount of nominal load, it would have twice the amount of capacitors, respectively.

Position of Banks: Two methods might be chosen for placement of capacitive compensation. The first one is lumping all banks at the same bus, for each area, in which the bus closest to the geometrical center at the main feeder is chosen. This means if 4 banks per area were selected at the previous step, now we insert all 4 banks at the very same place.

This enables simplification of installation and convenient access for maintenance. However, this also implies in bigger losses. A valid alternative herein proposed is to, instead, perform an unlumped distribution, dividing circa half of the load inside each area and perform a subsection within each area.

Next, performing a weighted average with the position of the loads, weighted with their apparent powers, inside each subsection, will result in an approximate localization for each bank. Figures 9 and 10 depict, with red crosses, the placement of the four banks throughout our system.

From that point, the closest bus on the main feeder is chosen. The main feeder is selected since it will provide the least distance when travelling to all other directions, whereas putting a capacitor further inside a ramification will only require the reactive power to travel back through the lines. Having in mind not all buses may be physically capable of having a capacitor bank installed, the closer to the main feeder the bank is installed, the better the result. The red arrows point the closest main feeder bus from the plotted crosses.

Attention is required as that the point drawn may not reflect in reality the shortest way represented; therefore, with aid of the distance map and knowledge of the grid disposition, it is possible to select which point will present the actual closest in case the point calculated is not accurately depicted due to the grid spatial geometry. An example of this is the mislead bus shown with a brown arrow, whereas the actual ideal bus is shown on red.

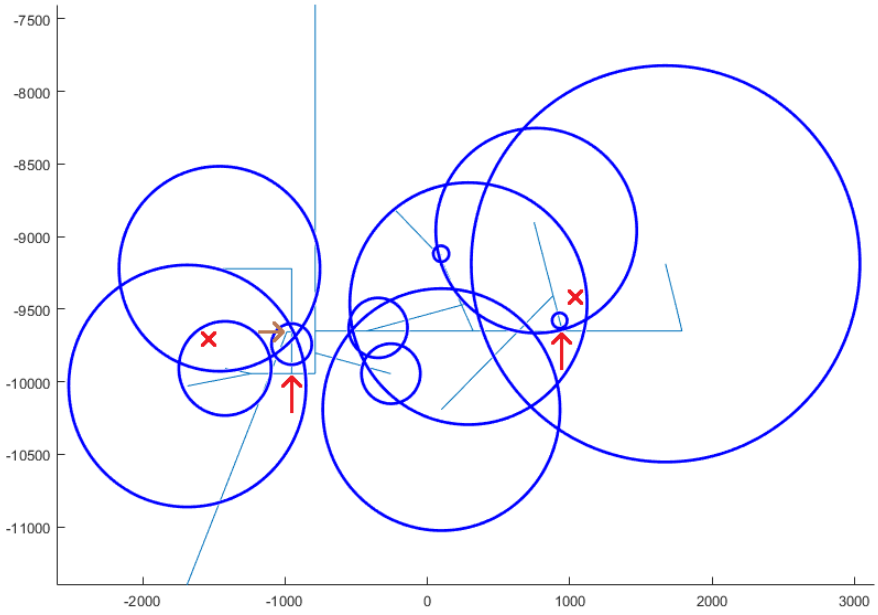

Figure 9: Position of weighted average results and nearest main buses on Area 1

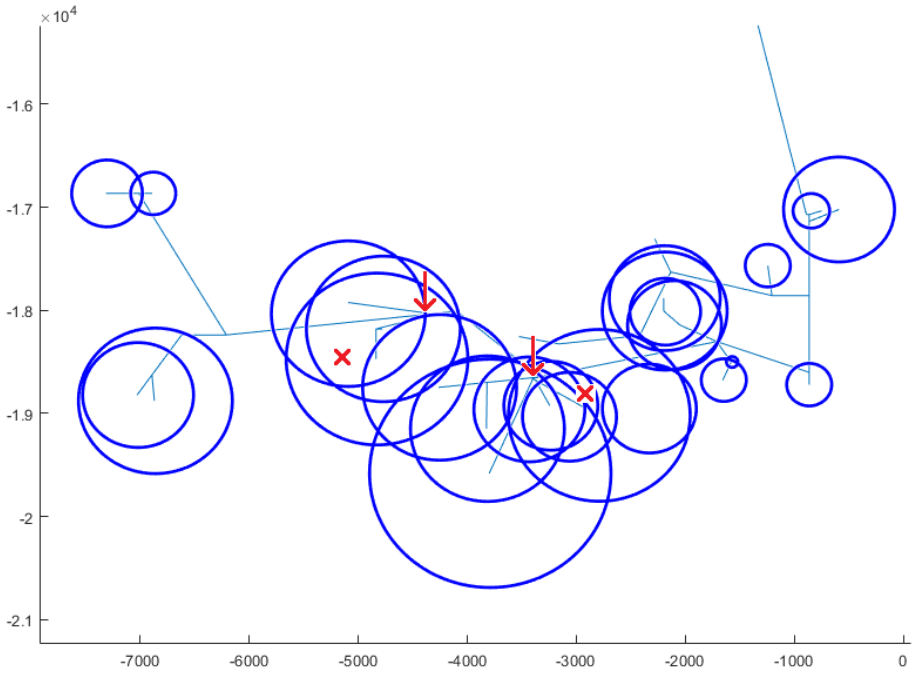

Figure 10: Position of weighted average results and nearest main buses on Area 2

5.1.2 Capacitor Sizing

iv) Reactive Power Determination

When determining the capacitive power to be installed at a system, there is a need to encompass more than only the inductive load of the circuit. To include losses and the circuit characteristics into account, such as transmission voltage drops through lines, a special power flow is executed. The power flow is executed in nominal power, and with only one capacitor bank. This bank is to be inserted on the end of the line. The reactive power of this capacitor, Q_T, will determine the reactive power of the final installation.

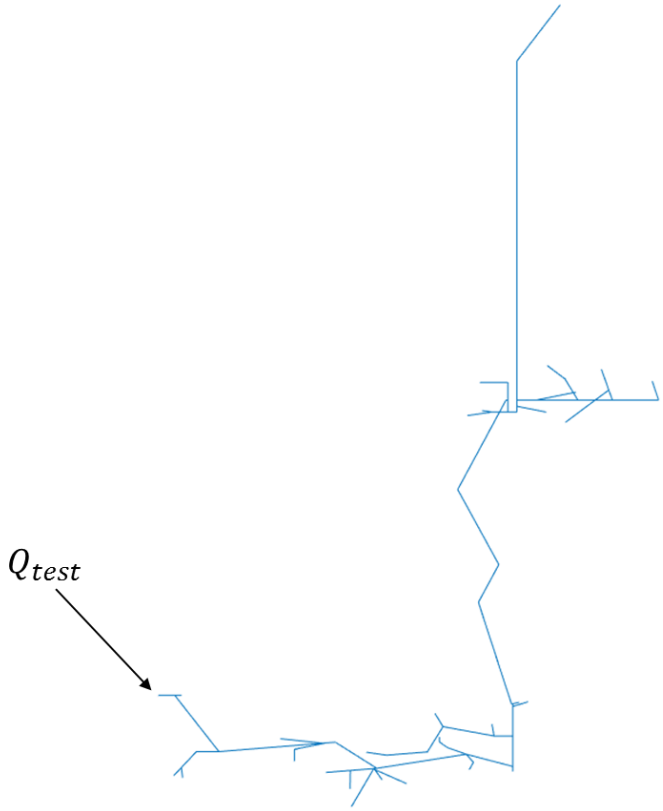

Figure 11: Position of test capacitor bank at end of circuit

To determine its value, power flows are executed while modifying the bank size. When the system bar with lowest voltage reaches 0.98 p.u., $Q_T = Q_{Min}$ is registered, and when the system bar with lowest voltage reaches 1.01 p.u., $Q_T = Q_{Max}$. The reactive power to be installed is, then, chosen so that $Q_{Min} \leq Q_T \leq Q_{Max}$. A fair choice is choosing an average value for Q_T.

This choice may include, at this point, consideration as for the available commercial values of capacitor banks. Additionally, the expansion of the grid may be regarded, including a desired factor e_f, multiplying Q_T.

For our case, considering no expansion factor ($e_f = 1$):

$$Q_T = e_f . \frac{Q_{Max} + Q_{Min}}{2} = 1. \frac{6250 + 7500}{2} = 6875\ MVAR$$

Rounding to a commercial number, we have Q_T = 7000 MVAR.

When calculating Q_{Max}, the reactive power flow through long cables or lines is to be observed. It may offer valuable information to assist the next steps.

v) Capacitor Sizing

The determination of the final values for each capacitor bank can be done in two different manners.

On the first, it is possible to divide the reactive power equally among all banks. This results in less costs for inventory and maintenance, since only one type of capacitor bank is used throughout the whole system; and it might simplify operations. It is important to remember, at this point, that areas with vast differences on local reactive powers should, therefore, have additional or less capacitor banks accordingly.

However, this might not render optimal losses values. If the designer chooses to select this equilibrated power allocation, then simply dividing the number of capacitors by the Q_T will result in each bank size.

Now, a second method will also be investigated, by focusing on determining which is the best combination to promote even functioning and low losses, within the available commercial capacitor values.

Initially, we distribute evenly Q_T in the total number of capacitors. For our case, that would lead to 4 banks of 1750 MVAR each. We will then perform a Load Flow simulation

and analyze the reactive power flow to better distribute the power between each bank.

We observe the power losses in the whole system, just as performed in Chapter 3; in this initial setup, we obtain 0.45 MW and 0.733 MVAR as losses. On a closer look at our circuit, we observe that there is a considerable reactive power flow between areas A_1 and A_2, of over 1250 MVAR. As described in Chapter 3, the long array of cables, with over 8000 feet, plays a big part on losses. Therefore, minimizing the reactive power flow between these areas would reduce the losses on the circuit.

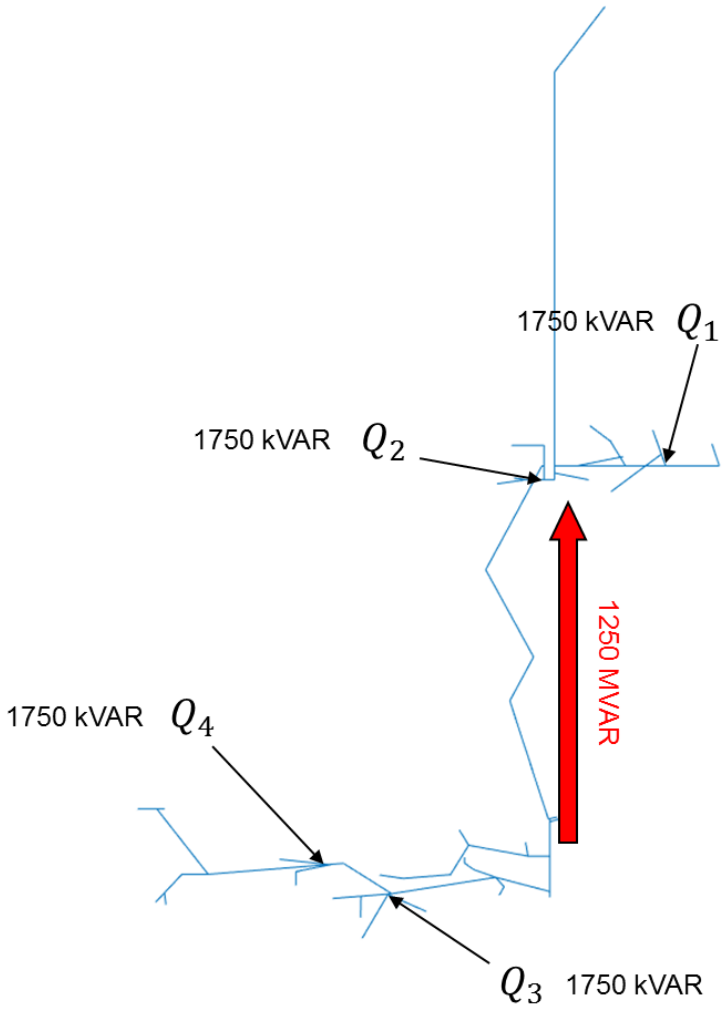

Figure 12: Demonstration of Power Flow imbalance analysis

At this moment, the step size for the capacitor banks will be set, admitting 250 kVAR per bank; this value is to be adopted as per requirement on usage of commercially available capacitor banks on the desired system.

Next, balancing the system with different values and writing down the power losses gives us Table X to compare these distributions of banks.

As seen on the table, there is very little difference between the cases in which the capacitors are balanced towards Area 1 (C_1, C_2 > C_3, C_4). This is due to the biggest loss of the circuit, through both areas, being balanced, and the minor differences of adjustment between different steps making the result all the same when taking into account the rest of the system.

Capacitor Banks (kVAR)				Power Losses	
C1	C2	C3	C4	P (MW)	Q (MW)
1750	1750	1750	1750	0.45	0.733
2250	2250	1500	1000	0.442	0.724
2250	2500	1500	750	0.442	0.724
2250	2250	1250	1250	0.442	0.724

Table 4: Capacitor Values vs Power Losses

The only noticeable difference is the unbalancing between the banks. This, however, will play a major role on next section, regarding the coordination of VAR Compensation. It is, therefore, favorable to pick the most balanced situation, in which the capacitors inside the same area are the same. This also reduces equipment costs.

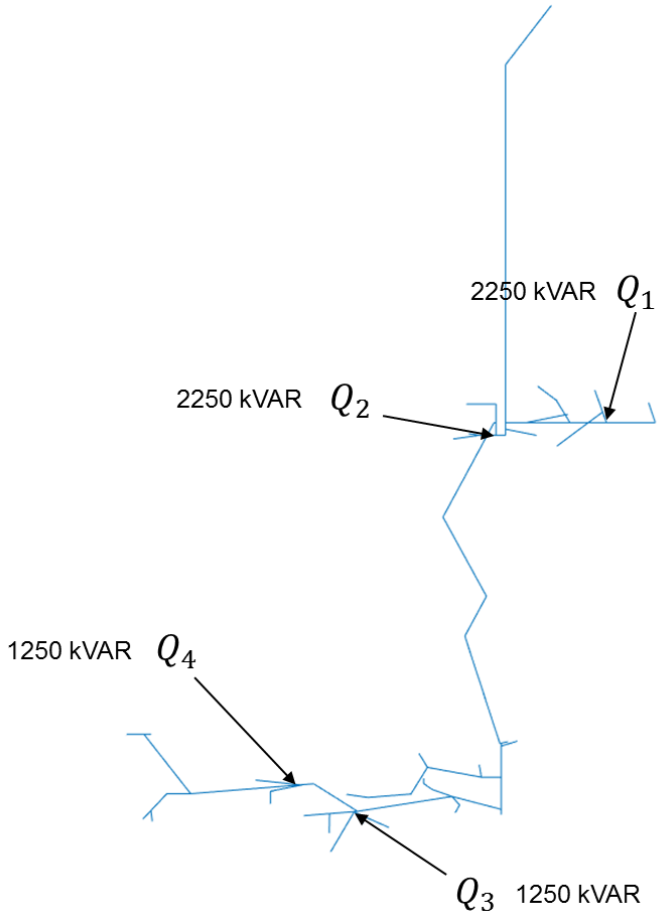

Figure 13: Final values of capacitor banks

Settling for this more even distribution of power between banks, seen on the bottom line of Graph X, the reactive power flow between A_1 and A_2 is lowered to 285 kVAR, flowing towards A_1, and the power losses are then set at the 0.42 MW, 0.72 kVAR, with a total efficiency of 93.82%.

Between the two methods, we will continue with this optimized, unbalanced distribution for the final application on this thesis. However, it is important to recall that either may be chosen, giving priority to lower maintenance costs and inventory, or lowering losses.

5.1.3 Switching Coordination

The final step on this method is to coordinate the operation of banks' switching to ensure proper coordination during any situation that may occur, whilst maintaining a minimal amount of switching realizations.

As we already chose a number of capacitors suiting minimization of actions, this step focuses on the voltage levels triggers and coordination between switches' activation.

At first, desirable voltage levels for grid maintenance are chose as 0.99 and 1.01 p.u., with standard values for hysteresis time and dead zones of 60 s. Simulations are run similarly to those on Chapter 4, on OpenDSS, and the following operation of Graphs 26 to 29 results from this preset.

Noticeably, we cannot ensure proper coordination at the present setup. In case we increase dead zones and hysteresis time, we still will have some undesirable effects.

On the other side, we have a reasonable tolerance margin within our voltage operation levels to work with. If we increase our margin and modify those levels to 0.99 and 1.02 p.u., we have the results seen on Graphs 30 to 33.

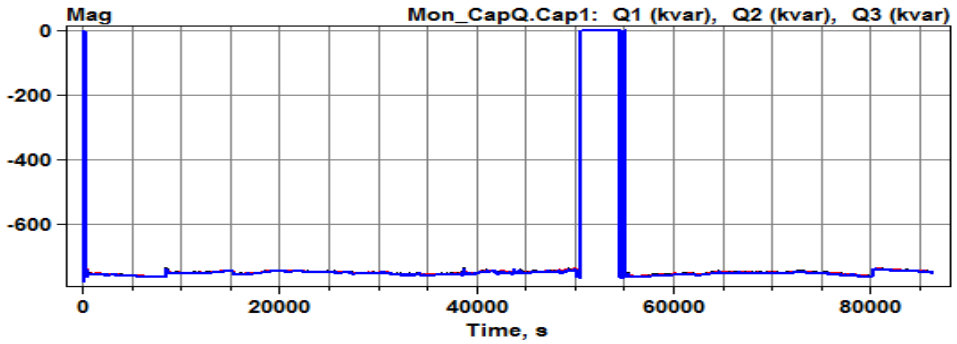

Graph 26: Capacitor Bank 1 Activation with 1.01 p.u.

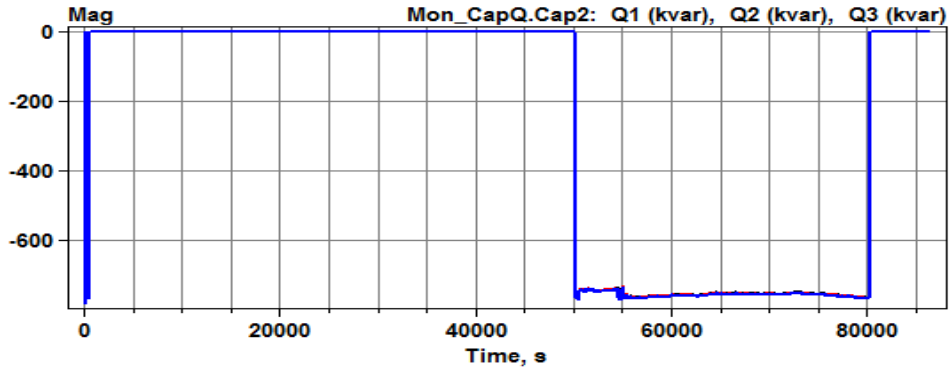

Graph 27: Capacitor Bank 2 Activation with 1.01 p.u.

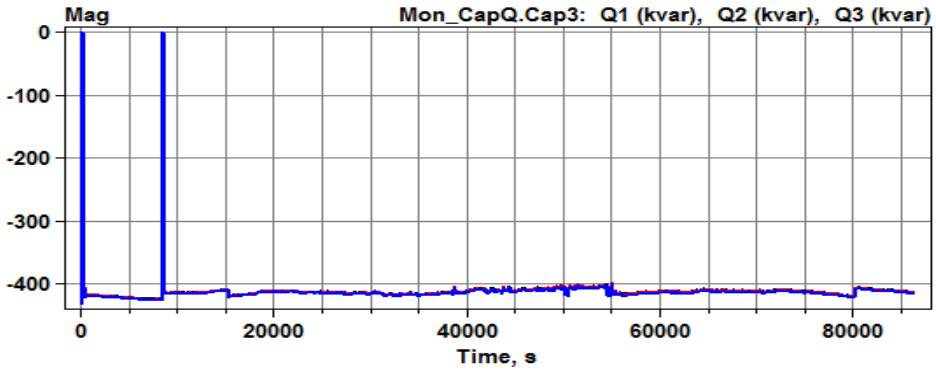

Graph 28: Capacitor Bank 3 Activation with 1.01 p.u.

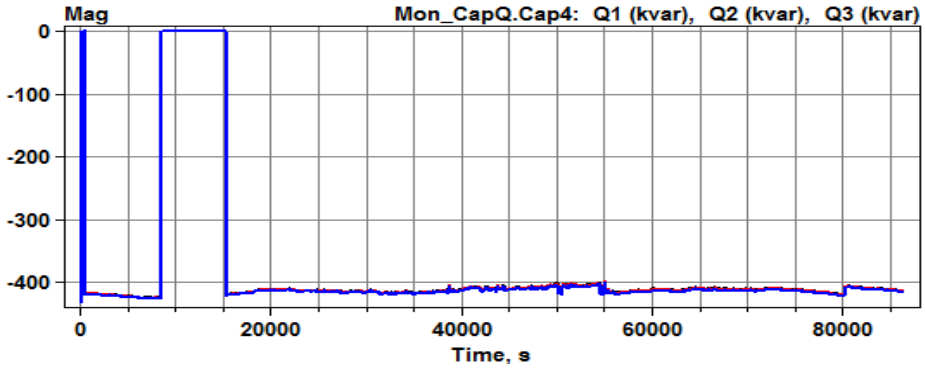

Graph 29: Capacitor Bank 4 Activation with 1.01 p.u.

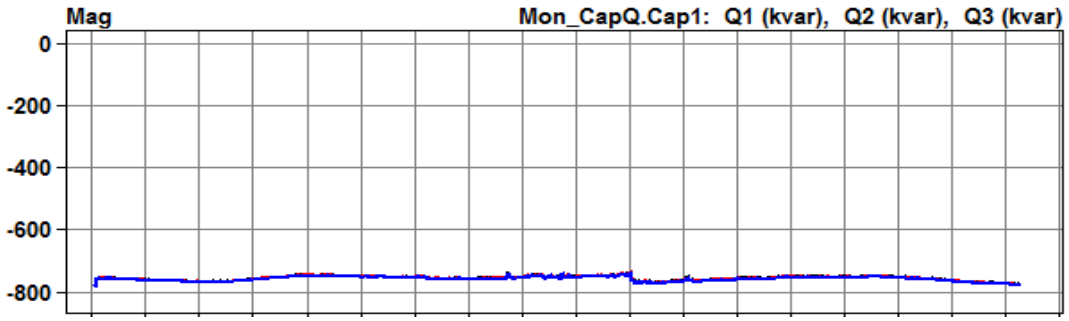

Graph 30: Capacitor Bank 1 Activation with 1.02 p.u.

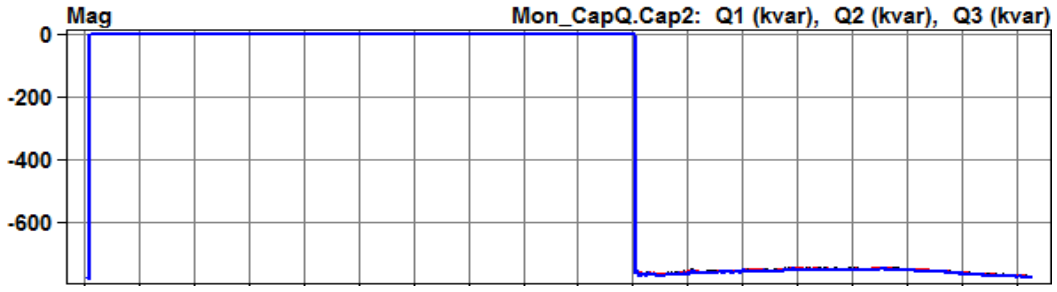

Graph 31: Capacitor Bank 2 Activation with 1.02 p.u.

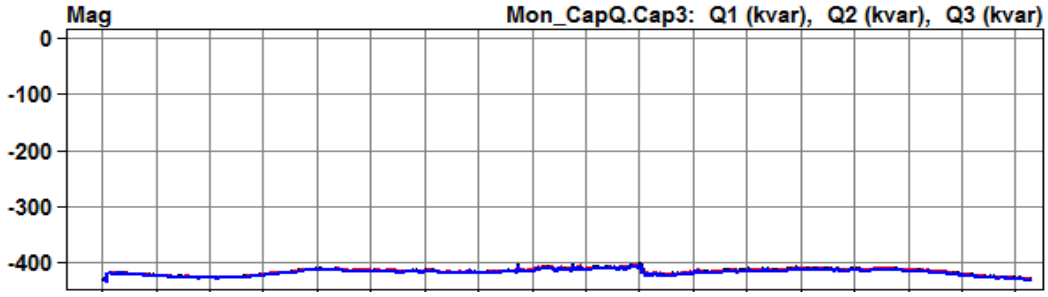

Graph 32: Capacitor Bank 3 Activation with 1.02 p.u.

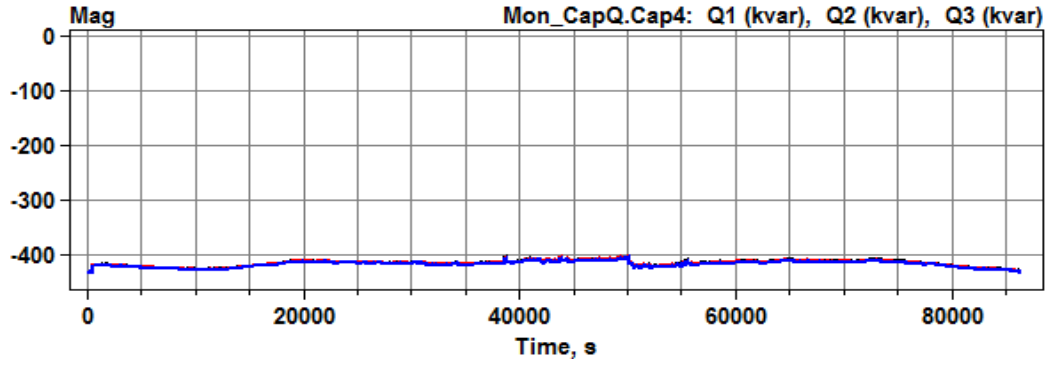

Graph 33: Capacitor Bank 4 Activation with 1.02 p.u.

At this moment, hysteresis time and dead zones have been kept at 1 minute each. Simulation of various load profiles might prove necessary a change on these properties, depending on the characteristic of the specific grid. It is recommended to change control levels at 0.01 p.u. steps, for each capacitor bank, increasing upper limits and decreasing lower limits separately. If the control cannot perform well within these conditions up to 1.04 and 0.96 p.u. margins, dead zones and hysteresis time must be increased to more than 60 s in 10 s steps, individually, while setting voltage control back to initial parameters, until convergence is reached for operation of the capacitors.

We perform additional sets of simulation without any solar generation, in which case the behavior is still operational and with no failures or undesirable operations during any moments.

5.2 Summary of Results

At Chapter 3, Table 3 shows the results from the 4-bank operation, in which case the losses were 463 kW and 759 kVAR. After applying the placement and sizing herein described, they had a reduction of 4.6% in real and imaginary losses, to 442 kW and 724 kVAR, and the system had an increase of efficiency from 93% to 94%.

The actual locations of the capacitor banks are different from the places proposed in this Chapter, as seen on Figure 2. Also, the value of 7000 MVAR for Q_T implemented in this method is smaller to that effectively in operation, which is 7200 MVAR. This means a reduction in costs, by using less reactive power to properly operate the grid. Furthermore, the similarities between these values and placement from original design reinforce the

validity of applying the novel method.

Moreover, the result from the switching operation during the time-sequence analysis was also very successful. When comparing to the performance obtained after tuning the proper control algorithm in Chapter 4, we see that it actually requires less switching operations, since the sizing of banks is optimized from the perspective of operation and placement. This reverts to less maintenance costs and overall grid efficiency increase.

On top of that, the performance of its operation in conjunction with power solar generation was perfect, and had no troubles whatsoever once the control has been correctly determined.

The steps required for implementation of this method are not complex, and enables users and designers to employ this methodology to create or modify reactive power compensation in power grids, whilst empowering the used by enabling smart decision making strategies based on the present scenario at hands.

6. STATIC VAR COMPENSATOR SIMULATION AND ANALYSIS

For each change a real transmission or distribution circuit has, throughout the day, a transient effect takes place. Every time we switch an electrical equipment connected to the grid, the characteristics that were stable change, and that effect might be undesired.

Therefore, not only our systems have varying conditions through time, but also transient responses to each of these changes. To lessen this effect, we might employ a number of different equipment and controls, so that the transient response is less intense, the steady state deviation is smaller, or even both.

Here, we will make use of a Static VAR Compensator (SVC), in conjunction with the previously studied methods. It will be installed on our system, and its effects and characteristics studied. The simulations are realized on the software ETAP 14.0.

Additionally, it is worth mentioning that SVCs may be employed at individual loads, or at a subgroup of loads, in order to enhance the power quality for that specific group. That way, less power would be required to provide similar results. However, this section will encompass the analysis of SVC usage for the system in general, meaning that similar results are perfectly achievable for groups of loads using the same techniques with smaller equipment.

6.1. Simulation Methodology

In order to properly test the effects of this equipment on this power system, we will utilize different actions that are present on normal operation, such as capacitor banks turning on or off. Besides that, we will have a total, instantaneous interruption of the solar

generation power plants.

This interruption does not happen in reality, as the transition takes at minimum some seconds (such as a dark cloud passing in front of the sun takes some time). However, we may use this results to enact the worst case scenario, an intermittency on the generation right at the point of most power produced (around 5 MW), which also could include a fault on the solar plants.

Therefore, we will simulate the following events, in this order:

- 10 s: Capacitor Bank 3 turns On;
- 13 s: Solar Generation Interruption (substation takes over load);
- 15 s: Capacitor Bank 2 turns On;
- 19 s: Capacitor Bank 2 turns Off.

Without any reactive power compensation, we can see the voltage of Graph 34 throughout the transient simulation. The bus analyzed on the results depicted on this chapter is an intermediate bus, located on the physical middle of the circuit.

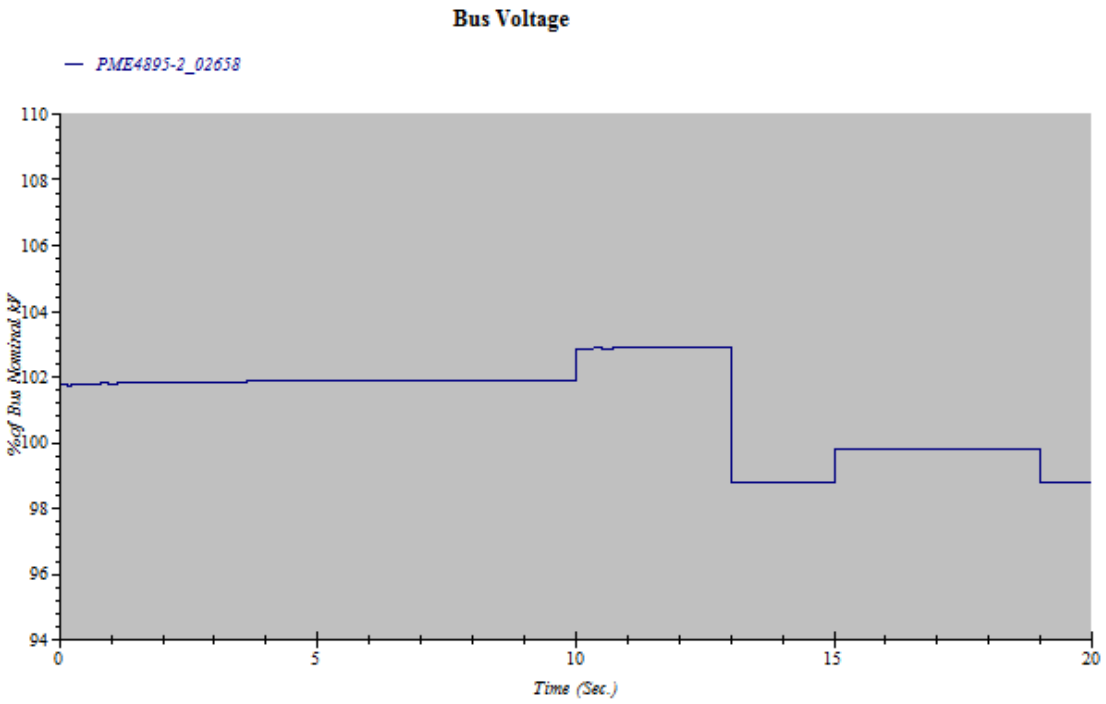

Graph 34: Bus Voltage without SVC

6.2. SVC Implementation

Now, this is clearly the case in all cases studied in Sections 3 and 4, where simulations took place on a system devoid of any kind of static VAR compensation. We can observe Graphs 14 and 21, representing the voltage on a passive system bus, and how much it changes through time, give all the circuits' variations. Depicted on Graph 34, we see the reason why: every time a circuit change takes place, there is an effect over the grid, which directly affects the voltage profile.

If we insert a very low rated module of a SVC, we will have the following result for the same sequence previously shown:

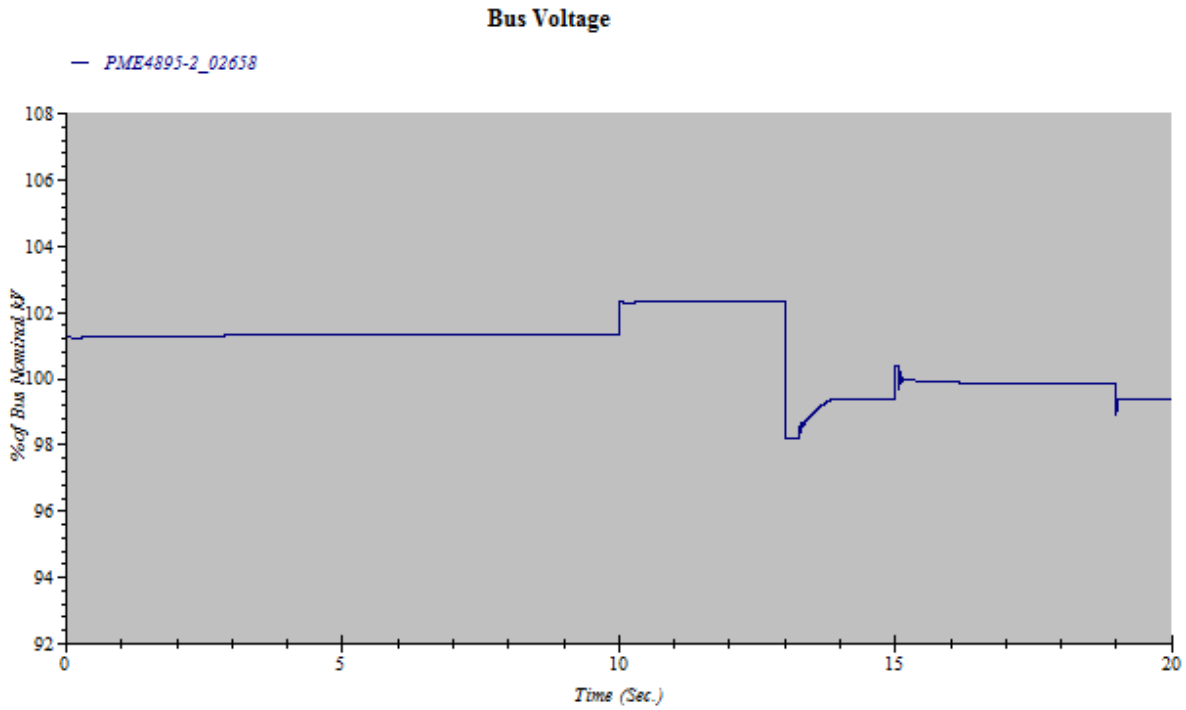

Graph 35: Bus Voltage with low-rated SVC

The harsh switching is still present, but we can already see some effect of the SVC on the line, taking place as the recovery of the system.

As we increase the rating of our equipment, we can see better effects on the grid

Graph 36: Bus Voltage with 1 MVAR SVC

stability. Results on Graph 36 show the effect of a 1 MVAR SVC, where the switching of the capacitor banks are very attenuated. There is still a noticeable voltage drop at the moment we cut off our solar power, however, in steady state, that effect is only 0.4%, from 1.002 to 0.998 p.u. at nominal voltage. Previously, we had a 4.1%, from 1.023 to 0.982 p.u., with a smaller equipment.

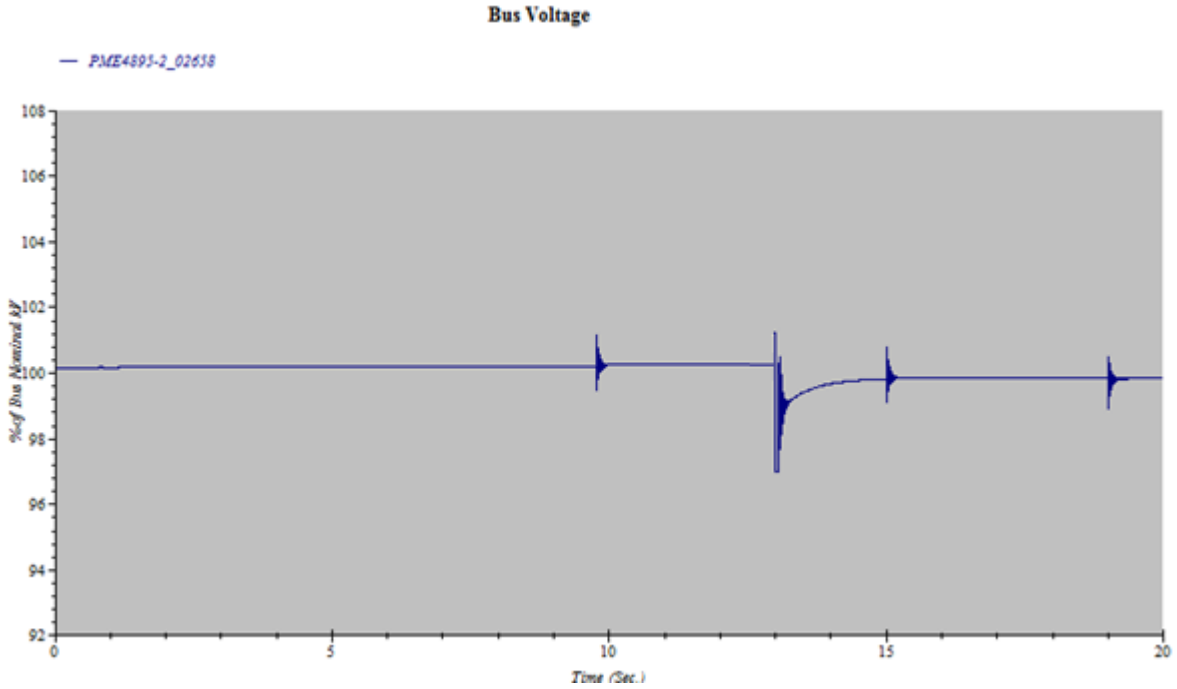

Next, on Graph 37, we see the results of a 2.5 MVAR SVC. We see that all transitions are less sharp than all previous cases, and that we have an almost constant 1 p.u. voltage at the selected bus.

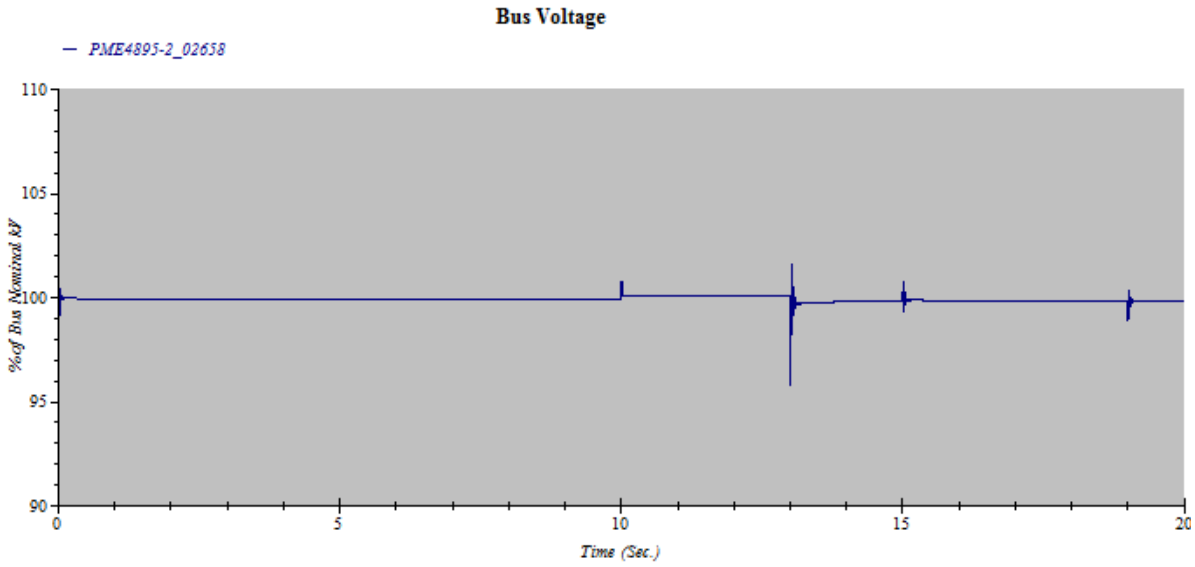

Graph 37: Bus Voltage with 2.5 MVAR SVC

Each equipment may be installed according to the requirements desired. In case we wish a high stability, with a high power quality throughout all our system, we may select the bigger equipment model as seen on Graph 37, which will alleviate the effects of all switching on the grid, through its technology.

In case we deem necessary to protect the system only of normal operations, such as capacitor switching, normal intermittency of solar power, and the normal load profile, we may select an SVC with a setting even lower than the capacitors present on the grid, as seen with results from Graph 36.

Additionally, smaller modules might be installed in particular sensitive loads, in case it is desired to improve only part of the circuit.

It is clear from the results that, for most regular transitions on daily operation, depicted on Graphs 3, 4 and 5, we might alleviate its transient impacts on the grid by using a 1 MVAR SVC.

6.3. SVC Optimal Positioning

There are many factors that determine the optimal placement for such a device. First and foremost, there are only a number of buses that can have such equipment installed. We cannot pick any of the buses throughout the system, as they may not have the infrastructure needed to install the device.

Secondly, the proximity to the system, and to the loads, can be taken into account. In case the system is either too close or too far from the power sources, we will have small effect of the system on our grid.

The voltage curve on Graph 38 is the result of placing a 1 MVAR SVC at the end of the circuit. We can notice, comparing to Graph 36, how less effective it was. The previously refrained capacitor

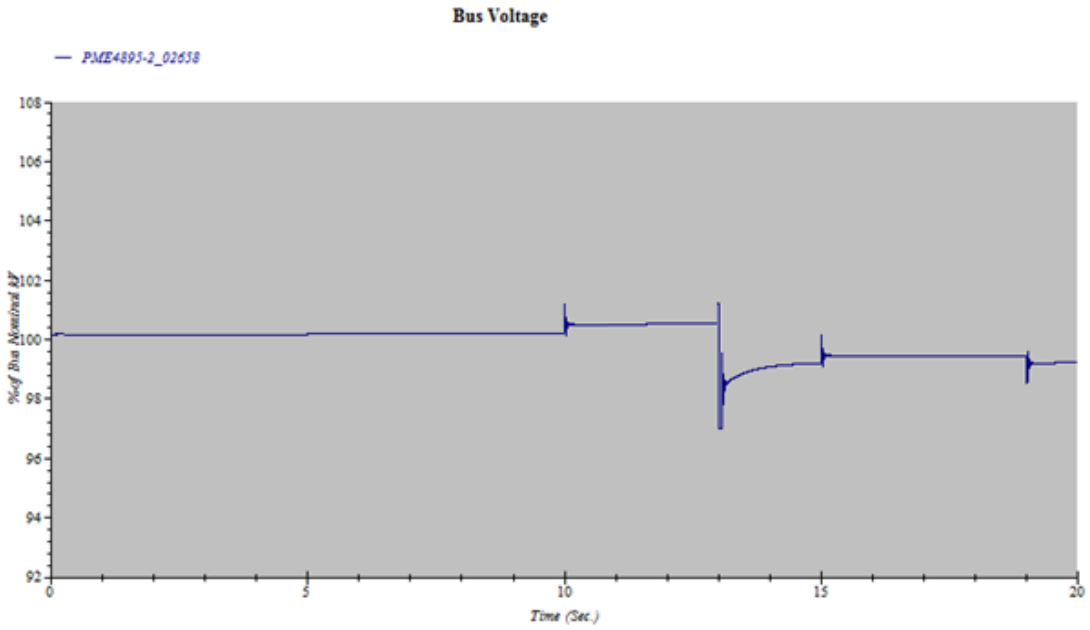

Graph 38: Bus Voltage with 1 MVAR SVC at circuit end

Similarly, in case we opt to position the SVC too close to the source, we will not have the desired effect either. On Graph 39, the SVC barely takes any effect from Capacitor Bank

#3, which is located too far away from the point in question. Also, the transient oscillation for the solar interruption event is smaller, but the steady state compensation is also less.

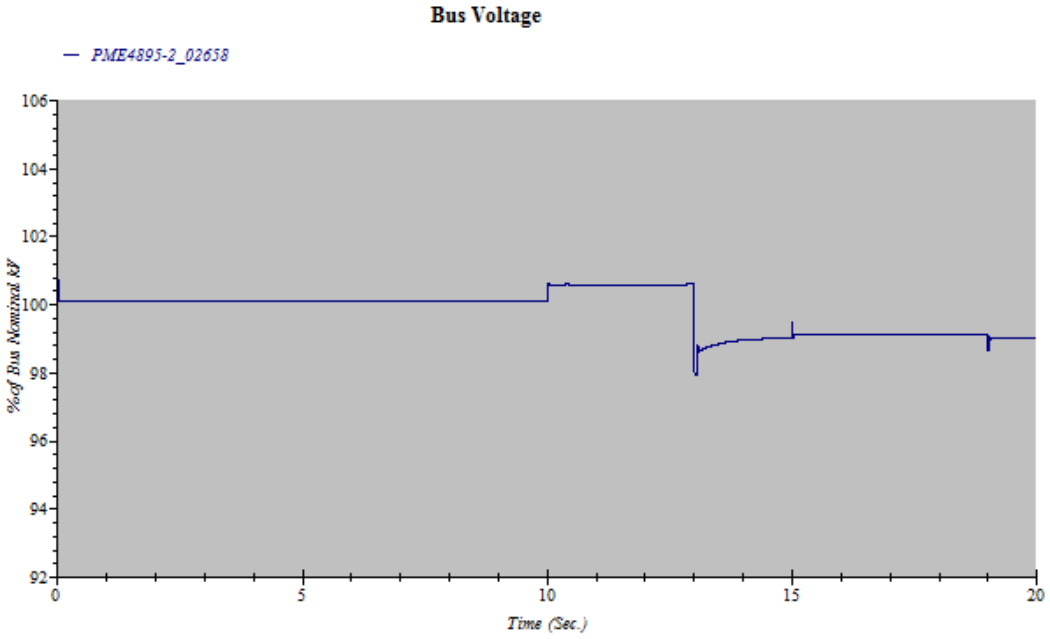

Graph 39: Bus Voltage with 1 MVAR SVC at circuit beginning

With this information, in conjunction with the previously studied effects of the different capacitor banks effects on the grid, we can narrow down the implementation of the SVC to the encircled area on Figure 14. That optimal placement will take place on a physically intermediate range, not too far away from the main desired disturbance point – the solar power plants and the capacitor banks.

Narrowing down our placement, according to Chapter 3, that position would be right before or right after Cable 9, prominent and noticeably. By doing so, we will be able to perform the stabilization for the majority of the loads. Physically, it is located at 18728 ft, or 5.7km - after the physical half of the circuit, but attending the majority of the loads.

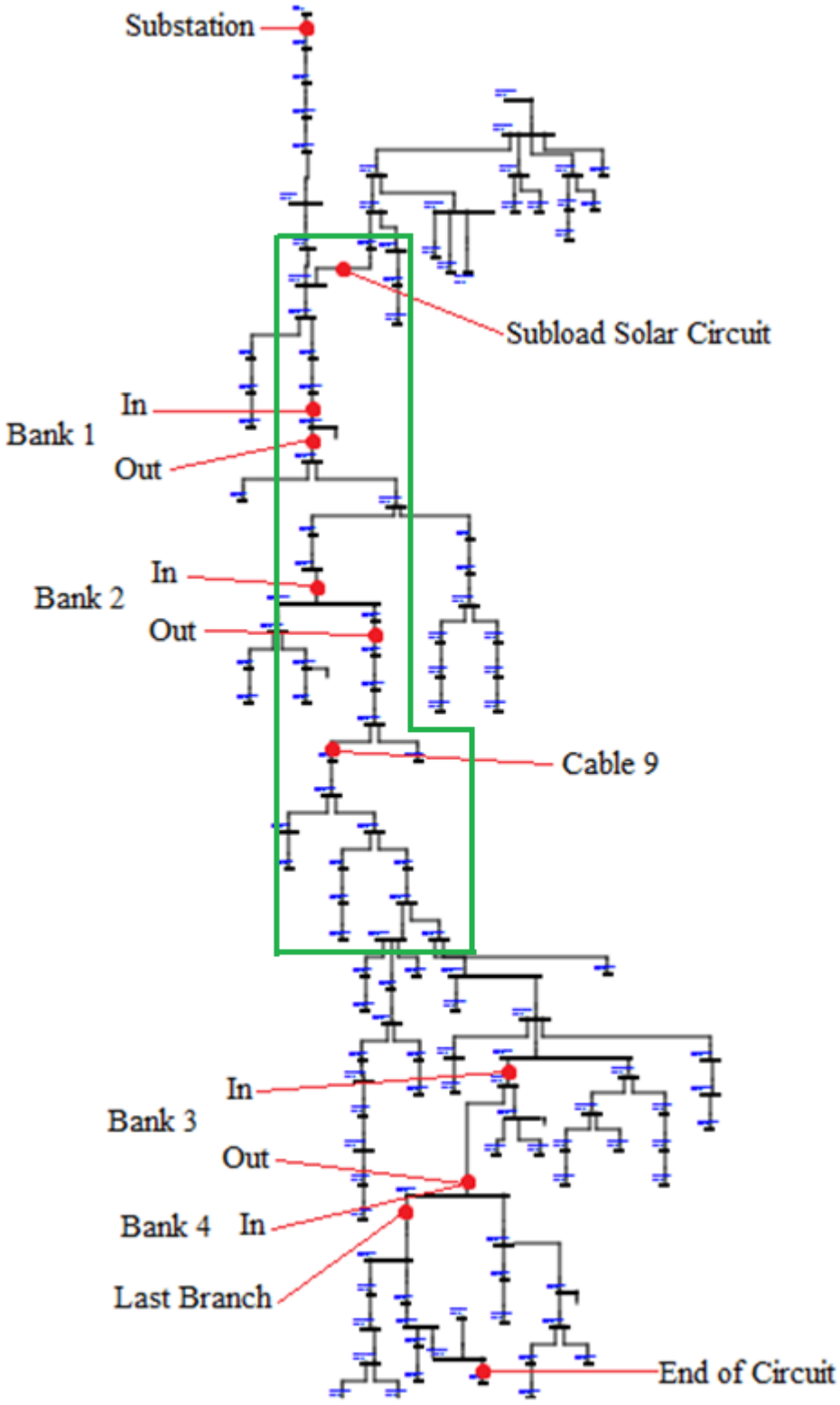

Figure 14: Optimal Positioning Region for SVC

If installed in the area preceding Cable 9, we will have similar effects throughout the grid. However, the further we place the SVC, the less effect it ought to have in the end-of-circuit loads. This way, we achieve a stabilization that is good for both the upper part and the lower parts of the circuit, as seen on Graph 40, where voltages of the initially analyzed middle-bus are shown in conjunction with the end of circuit (P5462488, in blue) and the start of circuit (W375, in red). We notice the effects are very similar, and the compensation is very effective throughout all the circuit extension.

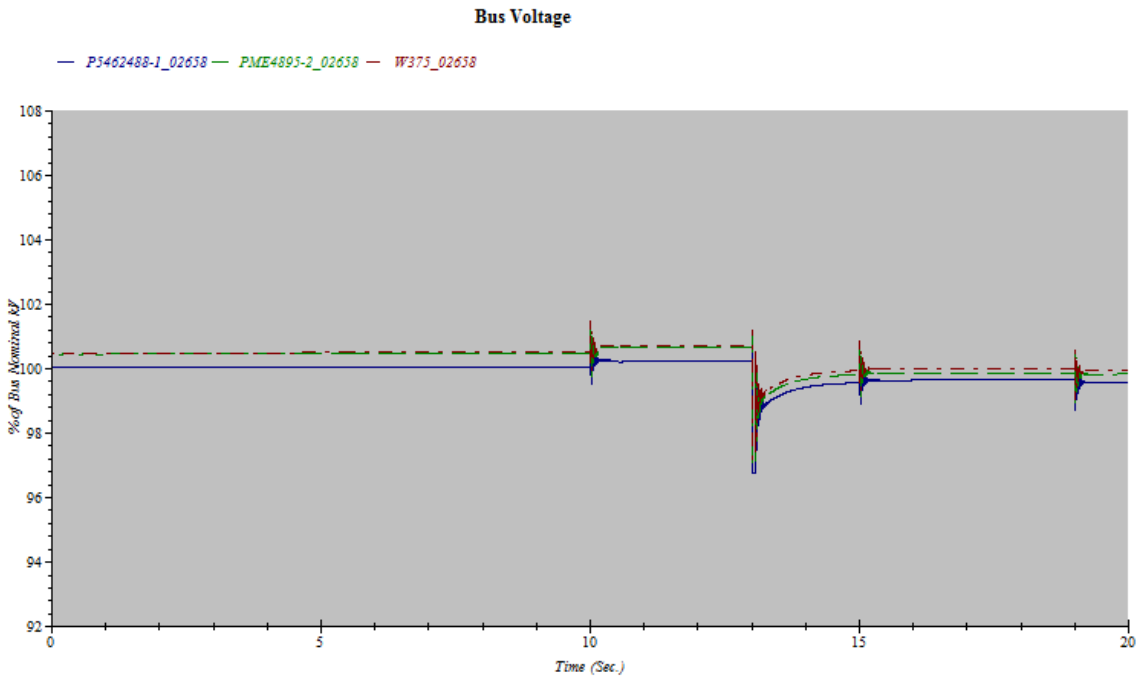

Graph 40: Buses Voltages with 1 MVAR SVC

It is worth noticing that, if desired, we may make use of more than one device. For instance, one at the depicted point, and another one closer to the solar power plants, responsible for compensating transients on their account, could suit the system's needs in case the operator wishes so.

Additionally, this position varies according to the circuit in question. If we had

different elements or placing for capacitor and solar plants, we would have different results for the optimal positioning.

6.4 Summary of Findings

On the same way we could determine effects of location on the usage of VAR Compensation techniques with capacitor banks at Chapter 3, we could also see differences and prioritize certain places when making use of SVC technology.

The waveforms were noticeably different, and the selection of a properly sized equipment would greatly affect power quality performance on the grid, under normal operation.

However, the dynamic transitions were still not accommodated. That means the SVC is not capable of coping with fast transients, present on everyday operations as well as – and specially at – faults and emergency situations. A possible solution for this is the use of Dynamic VAR controllers (DVC), such as the OCC-DVC [36].

7. CONCLUSION

The development of a new optimal capacitor placement and sizing technique was studied and implemented on a study grid, aiming losses reductions by employing graphical tools and power flow optimization; also, the thesis included the analysis of different cases of reactive power compensations implemented on a real circuit have been studied in this thesis.

On Chapter 3, we have analyzed the system operation at nominal power demand, investigating different capacitor banks combinations. After a thorough investigation, we identified the best scenario for the grid voltage level, and the two best scenarios for the lowest system losses. Moreover, we could identify that the location of the used VAR compensation was decisive for the system. Lastly, the possibility of utilizing methods such as VCR while still respecting the limits of operation from the system were discussed, as well as the respective advantages of operating the grid with lower voltage levels.

Subsequently, on Chapter 4, we simulated a load profile scenario, and implemented VAR Compensation in the form of capacitor banks under the presence of intermittent distributed generation. Even though there were very harsh spikes on the solar plants generated power, when properly programmed, the banks are turned on and off without falling into unresponsive or super-excited zones. By properly programmed, we understand that dead zones, hysteresis time, and voltage trigger points are set within levels that allow the proper functioning of the system, no matter which circumstance is in effect, in that particular system and its universe of possibilities.

The understanding brought by studying the grid in nominal load and daily profile

time-analysis simulations allowed a step further into VAR Compensation, resulting in a new approach to the capacitor placement problem. To perform a novel technique on design of reactive power compensation by switching capacitor banks, Chapter 5 covered power flow techniques in combination with graphical tools development to best determine location, sizing and switching algorithms to reduce losses. By employing techniques on simple software and user-friendly steps, along with specific criteria, it has been made possible to create a guideline for capacitor banks determination in power systems. The resulting technique was demonstrated in the very same power grid used in previous chapters, and the results were considerably similar. Additionally, a better efficiency was achieved versus the status quo by effectively reducing losses, as proposed by the technique herein described.

Finally, on Chapter 6, we studied the effect of a static VAR compensator, by installing a SVC in different places and scaling the power of modules in order to meet different criteria, from smaller to bigger reactive compensations, not on transient responses but steady state compensation. With a 2.5 MVAR SVC, we could oversee most of the effects that would normally impact our grid, and with a 1 MVAR we already saw drastic improvements.

We may observe the effects of different placement of VAR Compensation throughout the thesis. It is, therefore, possible to overcome negative effects related to renewable power generation from sources such as the intermittency of solar and wind power, as long as the pertaining situations are well defined and comprehended and adequate technologies are intelligently implemented and controlled to achieve stability, high efficiency and power quality.

Many suggestions rose from this study; to start with, photovoltaic inverters may be used for reactive power compensation, increasing both the availability of reactive power in

the power grid, and the usage of the inverters – which is normally limited by the weather conditions. As suggestion for next studies, including an inverter model capable of this operation will increase their usability [37].

Also as a suggestion, the Load shedding concept might be studied and implemented with the current generation curves. In addition to that, the usage of CVR and load shedding, combined with a well dimensioned VAR Compensation, may be able to control the grid in such a way that its renewable power generation has nearly no downsides.

Finally, the implementation of energy storage battery systems, whether in form of battery banks or fleets of plug-in electrical vehicles, can be also taken into account when performing studies on renewable power penetration. These add even more flexibility to our grid, allowing peak shaving, energy cost reduction, stable and smooth operation, among other benefits. It is, then, even more clear how it is necessary also to develop the power electronics equipment, which are the interface between the different energies connected in our grid.

BIBLIOGRAPHY

[1] F. Capra, *As Conexões Ocultas: ciência para uma vida sustentável*, 5th ed. São Paulo, Brazil: Cultrix, 2006.

[2] B. Nyamdash, E. Denny, "The causal relationship between GDP and electricity demand at a disaggregate level: A case study of Ireland," Energy Econ., 2010.

[3] ACNEEP, "The History of Energy Efficiency," January, 2013.

[4] ABB Inc, "Energy Efficiency in the Power Grid,", 2007.

[5] G. Walker, D. A. King, *O Tema Quente*: *como combater o aquecimento global e manter as luzes acesas*, Rio de Janeiro, Brazil: Objetiva, 2008.

[6] F. L. B. and A. I. Neto, "Matrizes energéticas no Brasil: cenário 2010-2030," XXVIII Encontro Nac. Eng. Produção, 2008.

[7] G. Arnold, "The Smart Grid: Power for the 21st century," Technologies Beyond 2020 (TTM), 2011 IEEE Technology Time Machine Symposium on, Hong Kong, 2011.

[8] K. Smedley and G. Smedley, "Power electronics enable energy super-highway," Power Electronics Systems and Applications (PESA), 2013 5th International Conference on, Hong Kong, 2013.

[9] R. F. Brena, C. W. Handlin and P. Angulo, "A smart grid electricity market with multiagents, smart appliances and combinatorial auctions," 2015 IEEE First International Smart Cities Conference (ISC2), Guadalajara, 2015.

[10] EV Volumes, "Global Plug-in Vehicle Sales for Q1-2016 and Preliminary April", available in http://www.ev-volumes.com/news/global-electric-vehicle-sales-2016-q1. Accessed on 10/13/2016.

[11] S. B. Peterson, J. F. Whitacre, and J. Apt, "The economics of using plug-in hybrid electric vehicle battery packs for grid storage," J. Power Sources, vol. 195, no. 8, pp. 2377–2384, 2010.

[12] J. Tomić and W. Kempton, "Using fleets of electric-drive vehicles for grid support," J. Power Sources, vol. 168, no. 2, pp. 459–468, 2007.

[13] Energy Information Administration, "How much Electricity Disappears between a Power Plant and Your Plug", available in http://insideenergy.org/2015/11/06/lost-in-transmission-how-much-electricity-disappears-between-a-power-plant-and-your-plug/. Accessed on 11/15/2016.

[14] E. Benedict, T. Collins, D. Gotham, S. Hoffman, D. Karipides, S. Pekarek, and R. Ramabhadran, "Losses in Electric Power Systems," Electr. Comput. Eng. Tech. Rep. - Purdue Univ., pp. 1–91, 1992.

[15] P. W. Sauer, "Reactive power and voltage control issues in electric power systems," Appl. Math. Restructured Electr. Power Syst. Optim. Control. Comput. Intell., pp. 11–24, 2005.

[16] J. Dixon, S. Member, L. Morán, J. Rodríguez, S. Member, and R. Domke, "Reactive Power Compensation Technologies : State-of-the-Art Review," vol. 93, no. 12, 2005.

[17] A. K. Sadigh, S. Member, and K. M. Smedley, “Review of Voltage Compensation Methods in Dynamic Voltage Restorer (DVR),” 2012.

[18] A. K. Sadigh, “Preparation of Power Distribution System for High Penetration of Renewable Energy”, Ph.D. Dissertation, University of California, Irvine, 2014.

[19] EATON, “Power Distribution Systems,” April 2016.

[20] Entergy, “Power Quality Standards for Electric Service,” June, 2008.

[21] R. Singh, F. Tuffner, J. Fuller and K. Schneider, "Effects of distributed energy resources on conservation voltage reduction (CVR)," 2011 IEEE Power and Energy Society General Meeting, San Diego, CA, 2011.

[22] W. Ellens, A. Berry and S. West, "A quantification of the energy savings by Conservation Voltage Reduction," 2012 IEEE International Conference on Power System Technology (POWERCON), Auckland, 2012.

[23] D. Gebbran, A. A. Alves, T. Cavalari, “Estudo De Viabilidade De Implantação Do Método Cvr Por Meio De Redes-Modelo Do IEEE”, Bachelors’ Thesis, Technological Federal University of Parana, Curitiba, Brazil, 2014.

[24] A. Grandjean, J. Adnot, and G. Binet, “A review and an analysis of the residential electric load curve models,” Renew. Sustain. Energy Rev., vol. 16, no. 9, pp. 6539–6565, 2012.

[25] J. P. Barton and D. G. Infield, "Energy storage and its use with intermittent renewable energy," in IEEE Transactions on Energy Conversion, vol. 19, no. 2, pp. 441-448, June 2004.

[26] EIA, “Today in Energy,” March 2013, avaiable in http://www.eia.gov/todayinenergy/detail.php?id=10211. Acessed at 12/14/2016.

[27] A. S. Siddiqui, F. Rahman, “Optimal Capacitor Placement to reduce losses in Distribution System,” WSEAS Transaction on Power Systems, vol. 7, January 2012.

[28] A. Sayed, H. Youssef, “Optimal Sizing of Fixed Capacitor Banks Placed on a Distorted Interconnected Distribution Networks by Genetic Algorithms,” IEEE Region 8 SIBIRCON, 2008.

[29] B. Gasbaoui, A. Chaker, A. Laoufi *et al*, “Optimal Placement and Sizing of Capacitor Banks using Fuzzy-Ant Approach in Electrical Distribution Systems,” Leonardo Electronic Journal of Practices and Technologies, issue 16, 2010.

[30] A. Elsheikh, Y. Helmy, Y. Abouelseoud, “Optimal capacitor placement and sizing in radial electric power systems,” Alexandria Engineering Journal, vol 53, December 2014.

[31] Y. Xu, Z. Y. Dong, K. P. Wong, E. Liu and B. Yue, "Optimal Capacitor Placement to Distribution Transformers for Power Loss Reduction in Radial Distribution Systems," in IEEE Transactions on Power Systems, vol. 28, no. 4, pp. 4072-4079, Nov. 2013.

[32] P. M. Sonwane and B. E. Kushare, "Optimal capacitor placement and sizing for enhancement of distribution system reliability and power quality using PSO," International Conference for Convergence for Technology-2014, Pune, 2014, pp. 1-7.

[33] R. Srinivasa Rao and S. V. L. Narasimham, “Optimal Capacitor Placement in a Radial Distribution System using Plant Growth Simulation Algorithm,” World Academu of Science,

Engineering and Technology, 2008.

[34] A.Y. Abdelaziz,E.S. Ali,S.M. Abd Elazim, “Optimal sizing and locations of capacitors in radial distribution systems via flower pollination optimization algorithm and power loss index,” Engineering Science and Technology, an International Journal, 2016.

[35] M. B. Liu, Claudio A. Canizares, W. Huang, “Reactive Power and Voltage Control in Distribution Systems with Limited Switching Operations,”, IEEE Transactions on Power Systems, 2008.

[36] L. Cheng, L. Xiangyang, S. Gaiping and W. Tao, "Study on Dynamic Voltage Conditioner with One-Cycle Control," 2006 International Conference on Power System Technology, Chongqing, 2006.

[37] M. Begovic, A. Pregelj, A. Rohatgi, D. Novosel, “Impact of Renewable Distributed Generation on Power Systems”, Proceedings of the 34th Hawaii International Conference on System Sciences on, Hawaii, 2001.

APPENDIX I

Example of OpenDSS interface

```
New linecode.mtxC116 nphases=3 BaseFreq=60
~ r1 = 0.000010
~ x1 = 0.000010
~ C1 = 0.000027
~ r0 = 0.000010
~ x0 = 0.000010
~ C0 = 0.000027
~ units=mi

New linecode.mtxC117 nphases=3 BaseFreq=60
~ r1 = 0.000010
~ x1 = 0.000010
~ C1 = 0.000027
~ r0 = 0.000010
~ x0 = 0.000010
~ C0 = 0.000027
~ units=mi

New linecode.mtxC118 nphases=3 BaseFreq=60
~ r1 = 0.000010
~ x1 = 0.000010
~ C1 = 0.000027
~ r0 = 0.000010
~ x0 = 0.000010
~ C0 = 0.000027
~ units=mi

New linecode.mtxC119 nphases=3 BaseFreq=60
~ r1 = 0.000010
~ x1 = 0.000010
~ C1 = 0.000027
~ r0 = 0.000010
~ x0 = 0.000010
~ C0 = 0.000027
~ units=mi

!Cable Codes: End


!*********************************************************************************************************************************************************************************************
!Cable Definitions: Start
!Number of Cables = 119.0

New Line.C1     Phases=3    Bus1=02658.1.2.3                Bus2=424E_02658.1.2.3                   LineCode=mtxC1      Length=1 units=mi
New Line.C2     Phases=3    Bus1=534E_02658.1.2.3           Bus2=98847880_02658.1.2.3               LineCode=mtxC2      Length=1 units=mi
New Line.C3     Phases=3    Bus1=98847880_02658_1.1.2.3     Bus2=P5574442-1_02658.1.2.3             LineCode=mtxC3      Length=1 units=mi
New Line.C4     Phases=3    Bus1=10839E_02658.1.2.3         Bus2=P5529630-1_02658.1.2.3             LineCode=mtxC4      Length=1 units=mi
New Line.C5     Phases=3    Bus1=4410836E_02658.1.2.3       Bus2=GS6969-3_02658.1.2.3               LineCode=mtxC5      Length=1 units=mi
New Line.C6     Phases=3    Bus1=GS6969-2_02658.1.2.3       Bus2=ND147897476_02658_C6End.1.2.3      LineCode=mtxC6      Length=1 units=mi
New Line.C7     Phases=3    Bus1=ND147897476_02658_C7Start.1.2.3    Bus2=ND152374261_02658.1.2.3       LineCode=mtxC7      Length=1 units=mi
New Line.C8     Phases=3    Bus1=ND152374261_02658.1.2.3    Bus2=GS6916-4_02658.1.2.3               LineCode=mtxC8      Length=1 units=mi
New Line.C9     Phases=3    Bus1=ND152374261_02658.1.2.3    Bus2=363E_02658.1.2.3                   LineCode=mtxC9      Length=1 units=mi
New Line.C10    Phases=3    Bus1=4123365E_02658.1.2.3       Bus2=ND54432662_02658.1.2.3             LineCode=mtxC10     Length=1 units=mi
New Line.C11    Phases=3    Bus1=ND54432662_02658.1.2.3     Bus2=ND136662598_02658.1.2.3            LineCode=mtxC11     Length=1 units=mi
New Line.C12    Phases=3    Bus1=ND136662598_02658.1.2.3    Bus2=S5010463T1_02658.1.2.3             LineCode=mtxC12     Length=1 units=mi
New Line.C13    Phases=3    Bus1=ND136662598_02658.1.2.3    Bus2=ND54432821_02658.1.2.3             LineCode=mtxC13     Length=1 units=mi
New Line.C14    Phases=3    Bus1=ND54432821_02658.1.2.3     Bus2=PME5672-1_02658_1.1.2.3            LineCode=mtxC14     Length=1 units=mi
New Line.C15    Phases=3    Bus1=ND54432821_02658.1.2.3     Bus2=RCS5187-3_02658.1.2.3              LineCode=mtxC15     Length=1 units=mi
New Line.C16    Phases=3    Bus1=RCS5187-2_02658_1.1.2.3    Bus2=P5464353-A_02658.1.2.3             LineCode=mtxC16     Length=1 units=mi
New Line.C17    Phases=3    Bus1=P5464353-B_02658.1.2.3     Bus2=P5464354-A_02658.1.2.3             LineCode=mtxC17     Length=1 units=mi
New Line.C18    Phases=3    Bus1=P5464354-B_02658.1.2.3     Bus2=P5465355-A_02658.1.2.3             LineCode=mtxC18     Length=1 units=mi
```

APPENDIX II

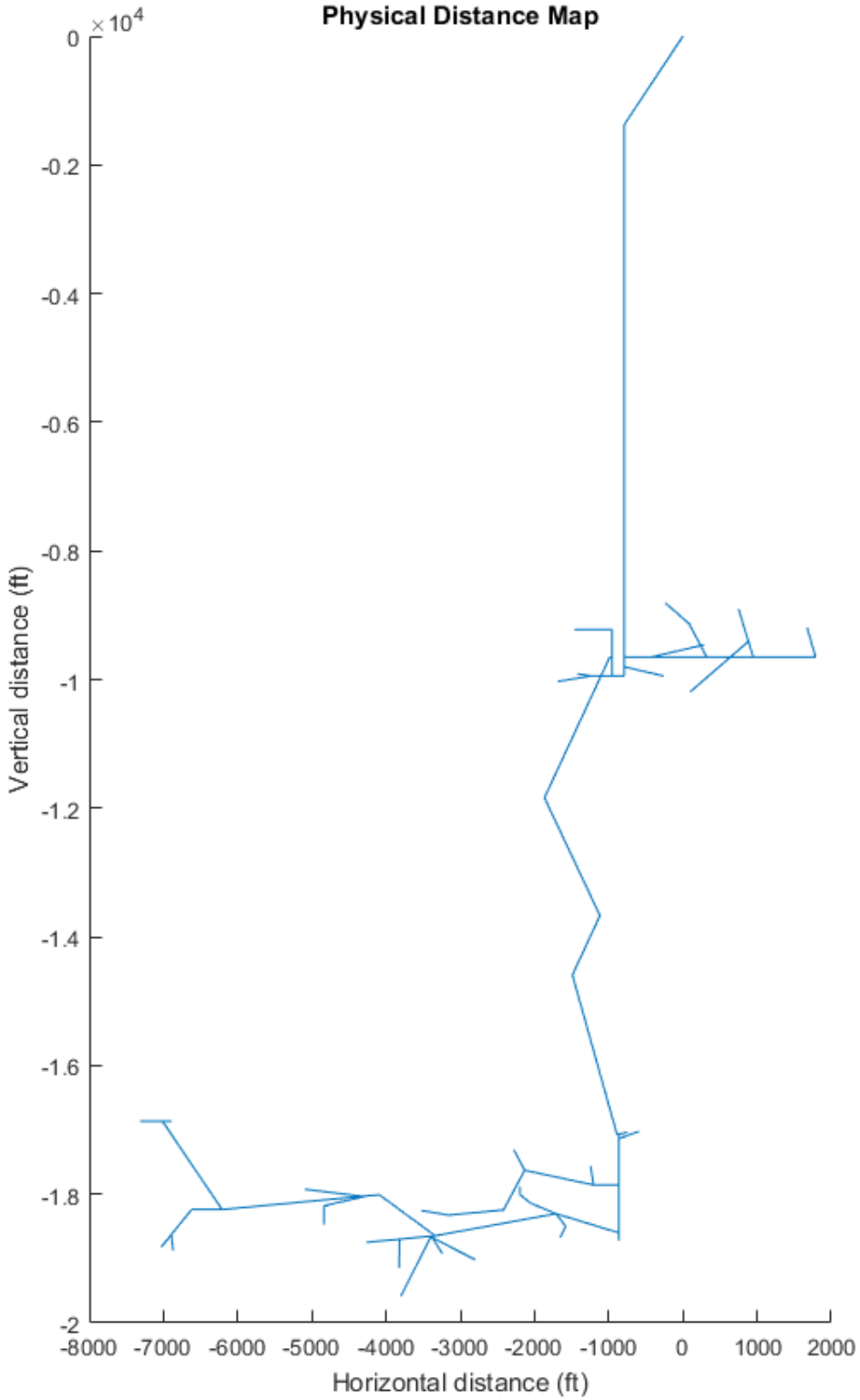
Physical Distance Map
×10^4
0
-0.2
-0.4
-0.6
-0.8
-1
-1.2
-1.4
-1.6
-1.8
-2
Vertical distance (ft)
-8000
-7000
-6000
-5000
-4000
-3000
-2000
-1000
0
1000
2000
Horizontal distance (ft)

APPENDIX III

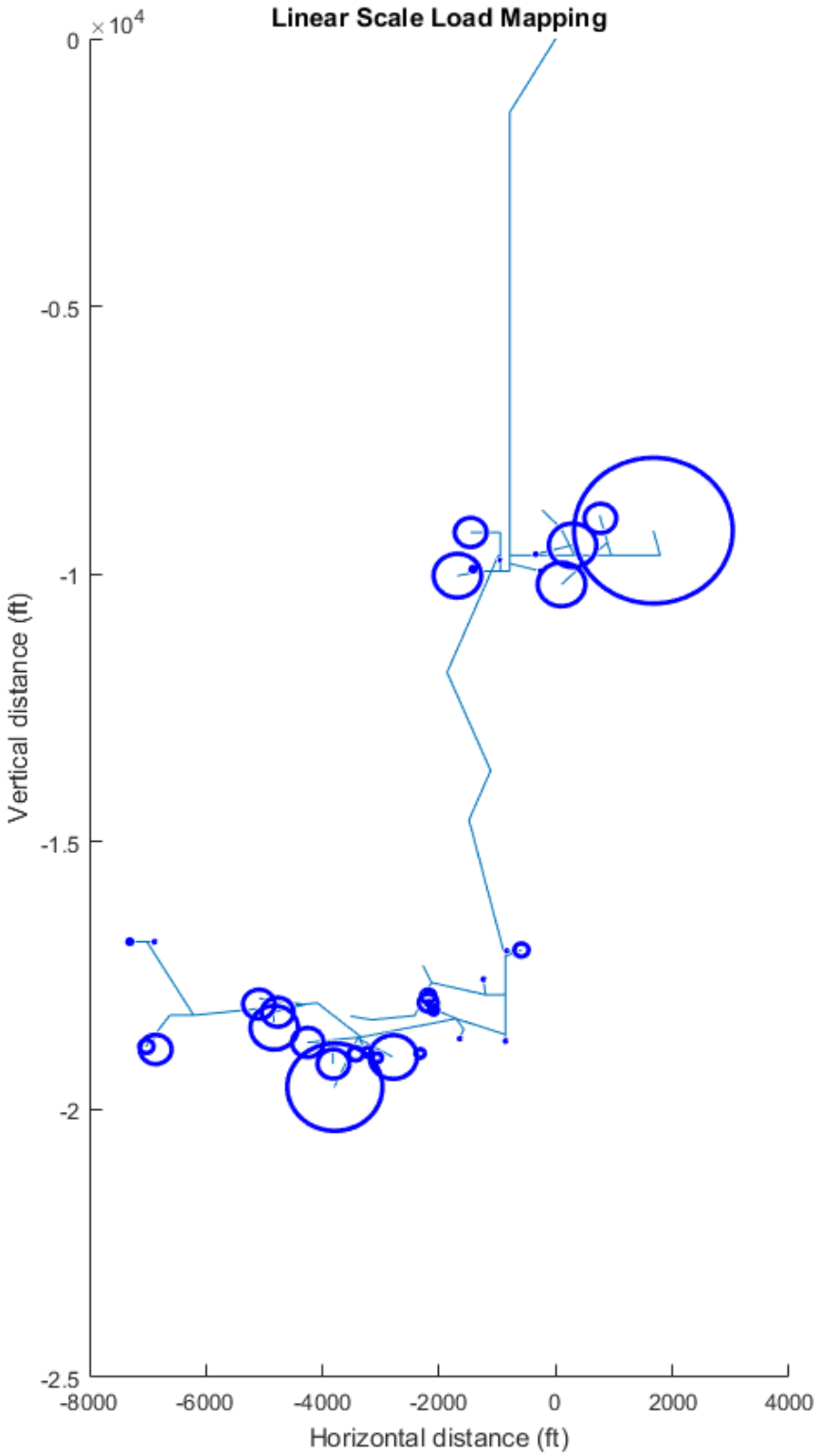

The following scales have been made with α = 0.29, 0.41 and 0.5, respectively, and with k = 0.18:

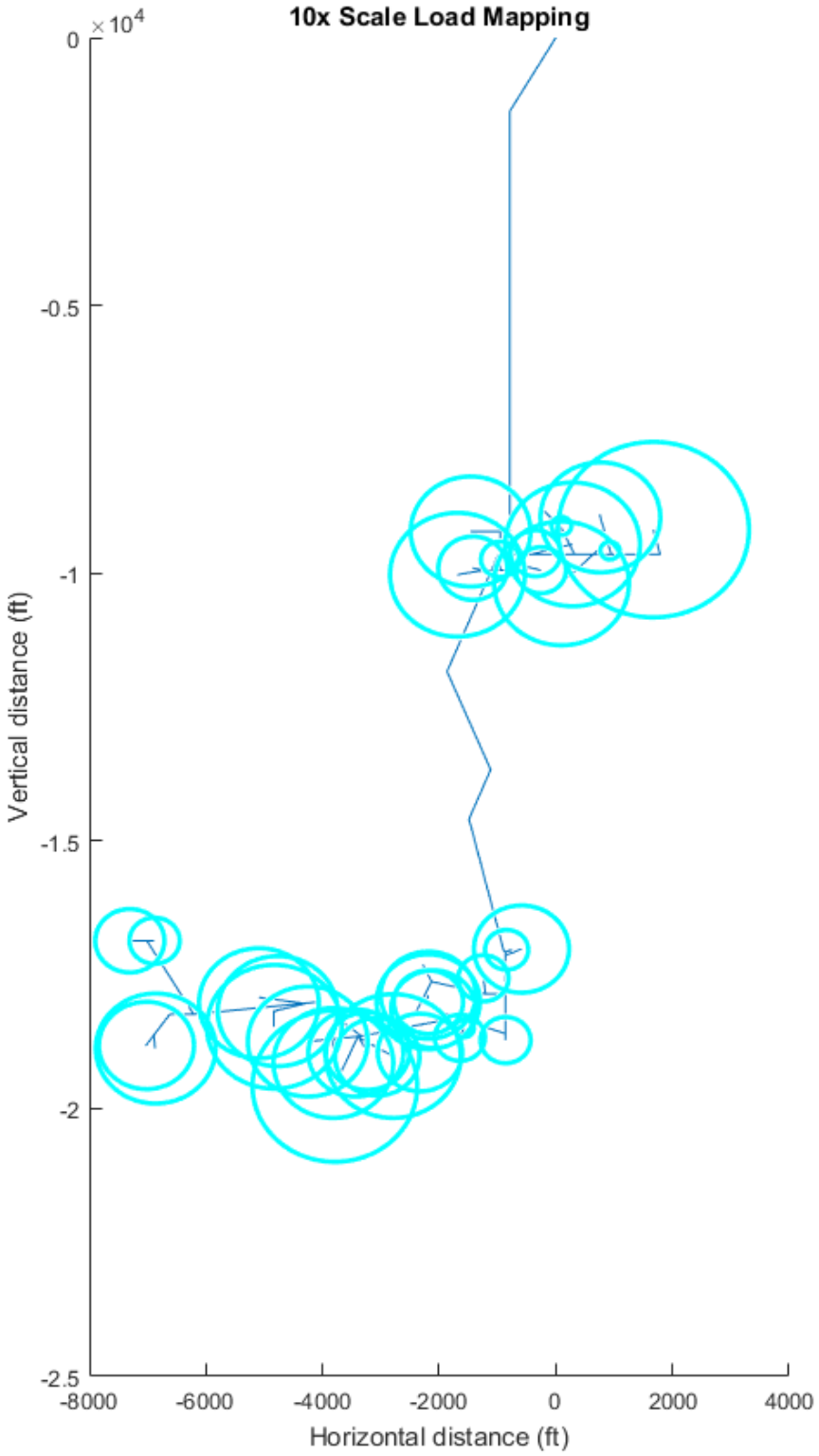

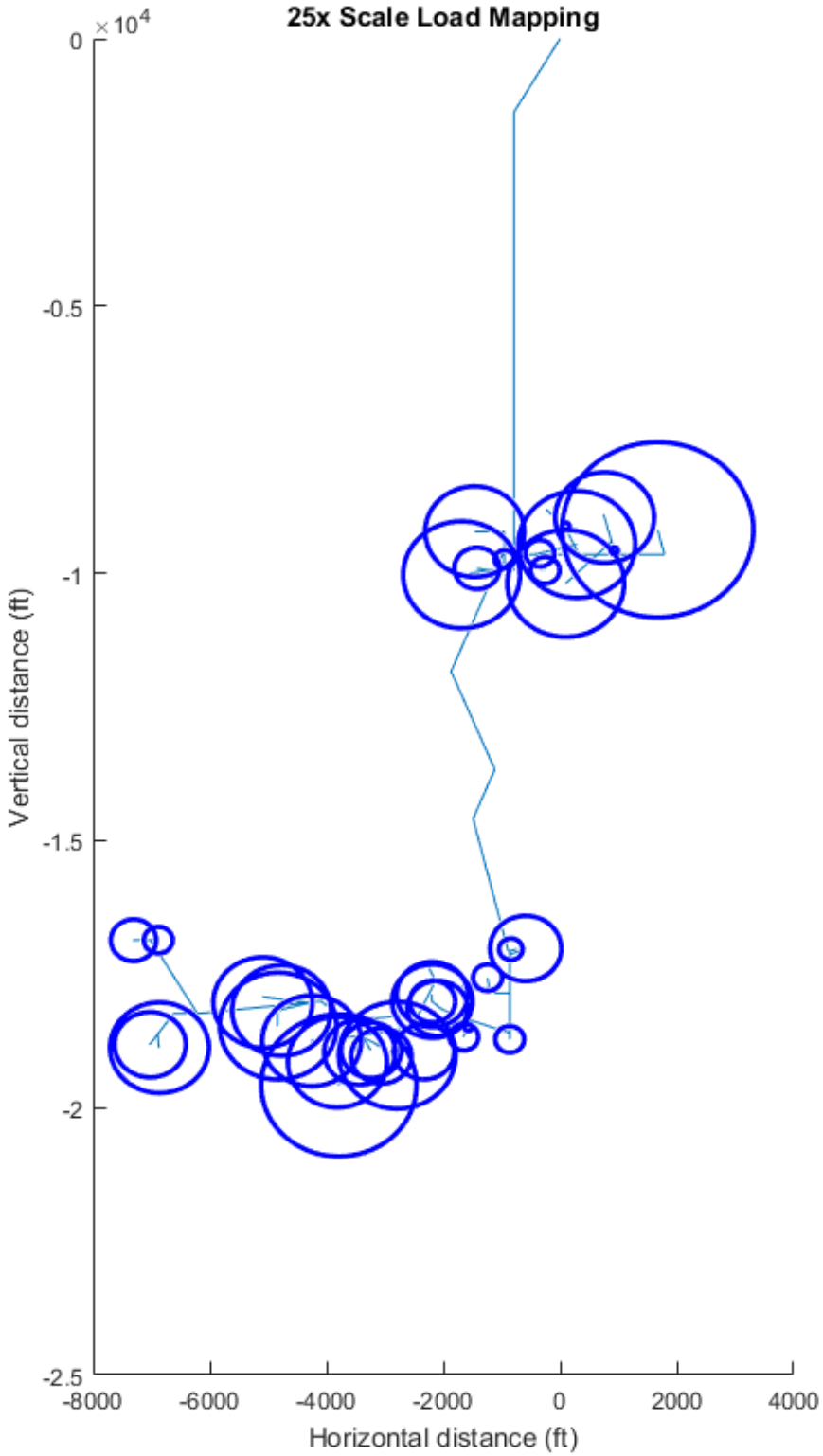
25x Scale Load Mapping
×10^4
0
-0.5
-1
-1.5
-2
-2.5
Vertical distance (ft)
-8000
-6000
-4000
-2000
0
2000
4000
Horizontal distance (ft)

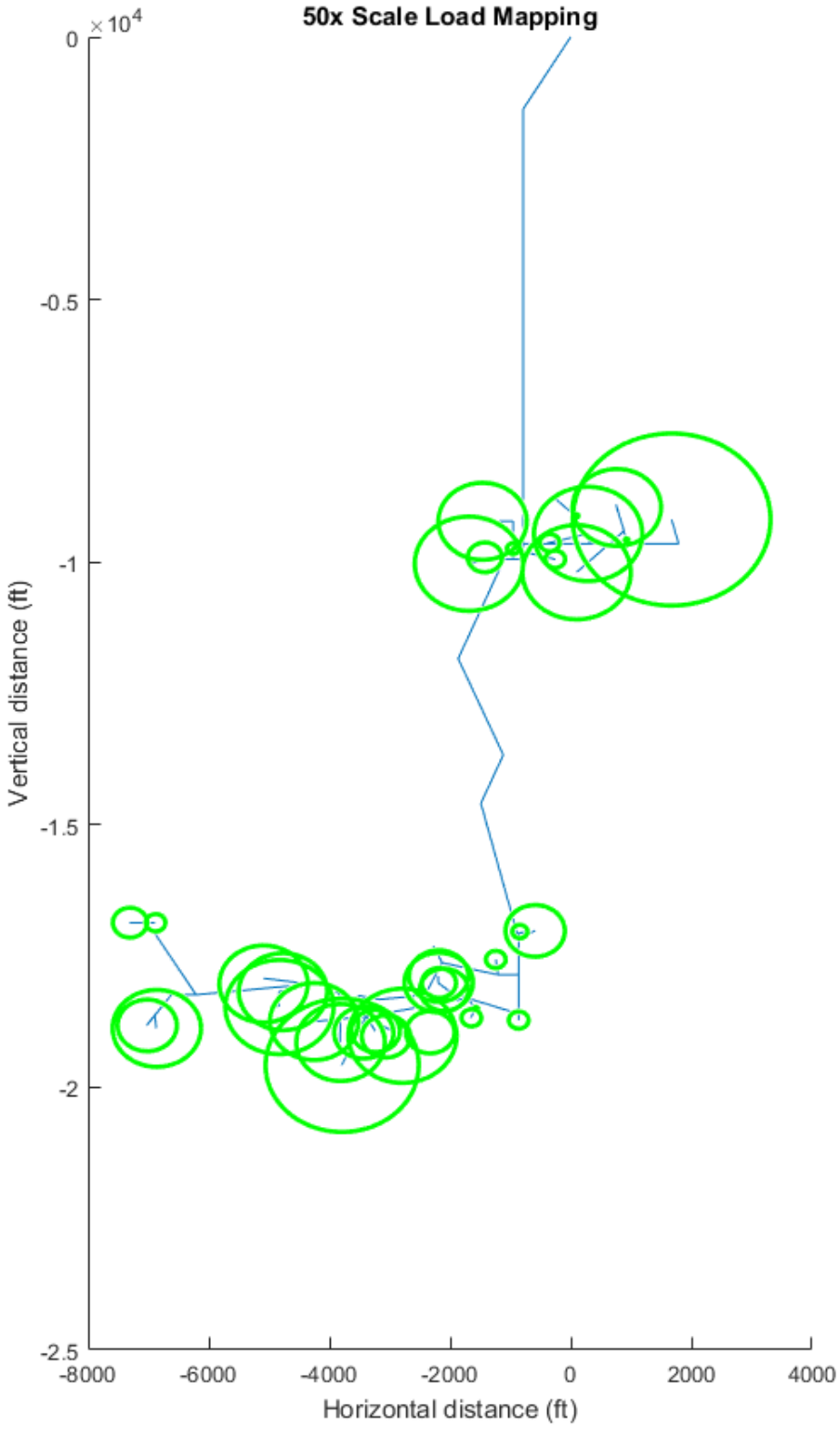
50x Scale Load Mapping
×10^4
0
-0.5
-1
-1.5
-2
-2.5
Vertical distance (ft)
-8000
-6000
-4000
-2000
0
2000
4000
Horizontal distance (ft)